Seasonal Dynamics of Soil Moisture Effects on Vegetation Productivity of an Oak Woodland Savanna and Grassland Ecosystem in Northern California

Théa C. Adumitroaie

ABSTRACT

Climate change continues to cause extreme weather patterns through droughts or excessive rainfall, affecting the functioning of terrestrial ecosystems. This study delves into the impacts of weather variation and soil moisture levels on the productivity of two distinct ecosystems: oak woodland savanna and grassland. It uncovers the variability and complexity in the relationship between soil moisture, vegetation productivity, and other environmental and biophysical variables, with a specific focus on energy balance fluxes and gross primary productivity (GPP) using eddy covariance data. In a wet year in an oak woodland savanna and grassland, the total amount of GPP assimilated over the growing season was 434.76 g C $m^{-2}d^{-1}$ and 135.10 g C $m^{-2}d$ respectively, with SWC ranging from 3.89% to 52.91% and 4.28% to 50.12%. In the dry year, the total amount of GPP during the growing season for the oak woodland savanna and grassland reached 348.96 g C $m^{-2}\ d^{-1}$ and 135.10 g C $m^{-2}\ d^{-1}$ respectively, with SWC ranging from 4.28% to 50.12% and 1.40% to 52.94%. Through an analysis of different MODIS products and their correlations with vegetation indices, the study offers critical insights into the dynamics of soil moisture and GPP. In the oak woodland savanna and grassland, soil moisture lagged 17 days and lagged 16 days in the wet year and 28 days and 12 days in the dry year respectively. Overall, these findings call attention to the resilience of the oak woodland savanna ecosystem to soil moisture changes, in contrast to the grassland's overall lower productivity and resistance. This research provides an updated analysis of two Northern California ecosystem responses to environmental changes, informing ecological management strategies for maintaining ecosystem functioning and resilience.

KEYWORDS

Water availability, eddy covariance, MODIS satellite data, ecosystem functioning, GPP

INTRODUCTION

Gross primary productivity (GPP) is the amount of carbon assimilated by photosynthesis at the ecosystem scale over time and is a critical component of the natural carbon cycle (O'Sullivan et al. 2020). Terrestrial ecosystems are a valuable tool in carbon sequestration of climate-warming anthropogenic emissions, since within the global carbon cycle, vegetation can sequester 30% of carbon dioxide emissions (Le Quere et al. 2018). The average global temperature is projected to increase between 0.3 and 4.8 °C by the end of the century (Stocker et al. 2013), and rising temperatures affect heat exchanges between terrestrial ecosystems and the atmosphere, driving the water transfer between the two through evapotranspiration. However, climate variability leads to large impacts on land carbon sinks globally (O'Sullivan et al. 2020). Ecosystem management benefits from extensive research on terrestrial biosphere-atmosphere feedbacks and how vegetation is affected by extreme dry periods driven by climate change, including how GPP is affected by soil moisture and energy exchange.

Analyzing vegetation dynamic changes, like the heat energy transferred between the canopy and the atmosphere that is driven by global temperature increases, can provide information on the ecosystem's hydrological cycle (Lian et al. 2021, Novick et al. 2016). Sensible heat is the radiative heat energy initially transferred between the canopy and the atmosphere and is mainly driven by the air temperature difference between the two. Latent heat is the heat energy transferred to the atmosphere through the phase change of water when evapotranspiration occurs, which drives the water transfer between the land and the atmosphere. These heat exchanges are central to the net radiation balance, which explains the energy partitioned between the solar or radiative energy absorbed by an ecosystem and the heat energy fluxes released into the atmosphere or deposited back into the soil (Chapin and Mooney 2002, Jung et al. 2011). When an ecosystem goes through dry periods with low soil moisture, plants must undergo physiological adjustments such as stomatal conductance, or the opening and closing of the plant's stomata, which helps moderate carbon uptake (O'Sullivan et al. 2020, Chen et al. 2017).

To observe these changes on a larger scale, we can analyze the structural changes of the different ecosystem types containing trees or solely grasses. It can be easier to observe structural changes in grasses, which under a Mediterranean climate dry out and senesce over the summer and are greatly controlled by precipitation patterns and variability (Gherardi and Sala 2015). Increased rainfall variability causes vegetation productivity and overall biomass of a grassland ecosystem to increase in the wet years. Extreme dry periods following the wet year increase fire risk with a decrease in soil moisture and an accumulation of residual dry matter. Understanding the implications of seasonal dynamics and soil moisture dry-down timing in an ecosystem can inform land management planning to most effectively preserve biodiversity through highly detailed ecological descriptions for management strategies such as grazing rotations and prescribed burning regimes.

The seasonal dynamics and relationships between these environmental variables can be studied using two observational methods – eddy covariance and satellite remote sensing– in order to provide a holistic analysis with varying spatial and temporal resolutions. GPP is not directly observable on a large scale, but proxy measures of terrestrial ecosystems provide pieces of information to infer productivity. Combining several vegetation observation methods increases the efficacy and accuracy of the data analysis process (Mohammed et al. 2019). Analyzing relationships of GPP to soil moisture changes from different spatial and temporal scales provides a robust analysis of soil moisture availability on plant productivity. Plant transpiration is an energy-driven process and plays a crucial role in determining GPP levels. Energy flux information collected through *in-situ* land-based tower observations and satellite-based methods is useful for observing changes in soil water content and its effects on GPP levels on a seasonal scale. Eddy-covariance flux towers are located in the Northern California region of study, which includes an open grassland and oak woodland savanna (Xu and Baldocchi 2003). Eddy-covariance data provides observations of the heat flux exchanges and soil moisture at high temporal resolutions, whereas surface reflectance data taken from satellites like MODIS investigate vegetation health and photosynthesis fluctuations (Mohammed et al. 2019).

Here, I explored the impacts of weather variation driven by climate change and differing levels of soil moisture on the productivity of an oak woodland savanna and grassland. My main question asks: How does vegetation productivity (GPP) respond to seasonal fluctuations of soil moisture in an oak woodland savanna and grassland in Northern California? To answer this question, I address three specific questions: (1) How does energy balance relate to productivity on a seasonal scale? (2) How does soil moisture availability affect photosynthesis in these two regions? (3) How does soil moisture affect GPP response timing in a wet year versus a dry year?

I expect that there will be heightened levels of sensible heat exchange in the Tonzi ranches compared to the Vaira ranches due to differences in vegetation types and different water acquisition strategies from the soil (Baldocchi et. al 2004). Tonzi Ranch, which contains an overstory of blue oaks, is more robust to experiencing changing conditions due to this vegetation type's seasonal behaviors. Whereas the Vaira Ranch, which contains grasslands, is much more sensitive to dry conditions as grasslands tend to completely die and become unproductive during the summer months. With decreasing water availability, I expect that the vegetation present in the Tonzi region will show higher levels of plant productivity compared to the Vaira region. Grasses and woodlands differ in photosynthetic strategies and root length for water acquisition methods. This makes the oak woodland savanna vegetation at Tonzi more robust to soil moisture fluctuations and water-limited conditions leading to higher vegetation productivity and resilience during stressful conditions in contrast to Vaira.

METHODS

Site Description

The Tonzi Ranch site is located in the lower foothills of the Sierra Nevada Mountains in Northern California (latitude: 38.431 °N; longitude: -120.966 °S), with the vegetation present classified as oak savanna woodlands (Figure 1). This site contains an overstory of blue oak trees (*Quercus douglasii*) and an understory of grasses (Baldocchi et al. 2004). The growing season is confined to the wet season, typically from October to May.

Located 3 km away in the lower foothills of the Sierra Nevada Mountains is the Vaira Ranch site (latitude: 38.413 °N; longitude: -120.951 °S) (Figure 1). This site is dominated by C3 grasslands including *Brachypodium distachyon L., Hypochaeris glabra L., Trifolium dubium Sibth., Trifolium hirtu*, which are known to not undergo separate light and dark reactions in photosynthesis to regulate plant transpiration (Baldocchi et al. 2020). Growing season is also confined to the wet season, from October to early May. The Mediterranean climate has rainfall contained between October and May, with little to no rain occurring during the summer months.

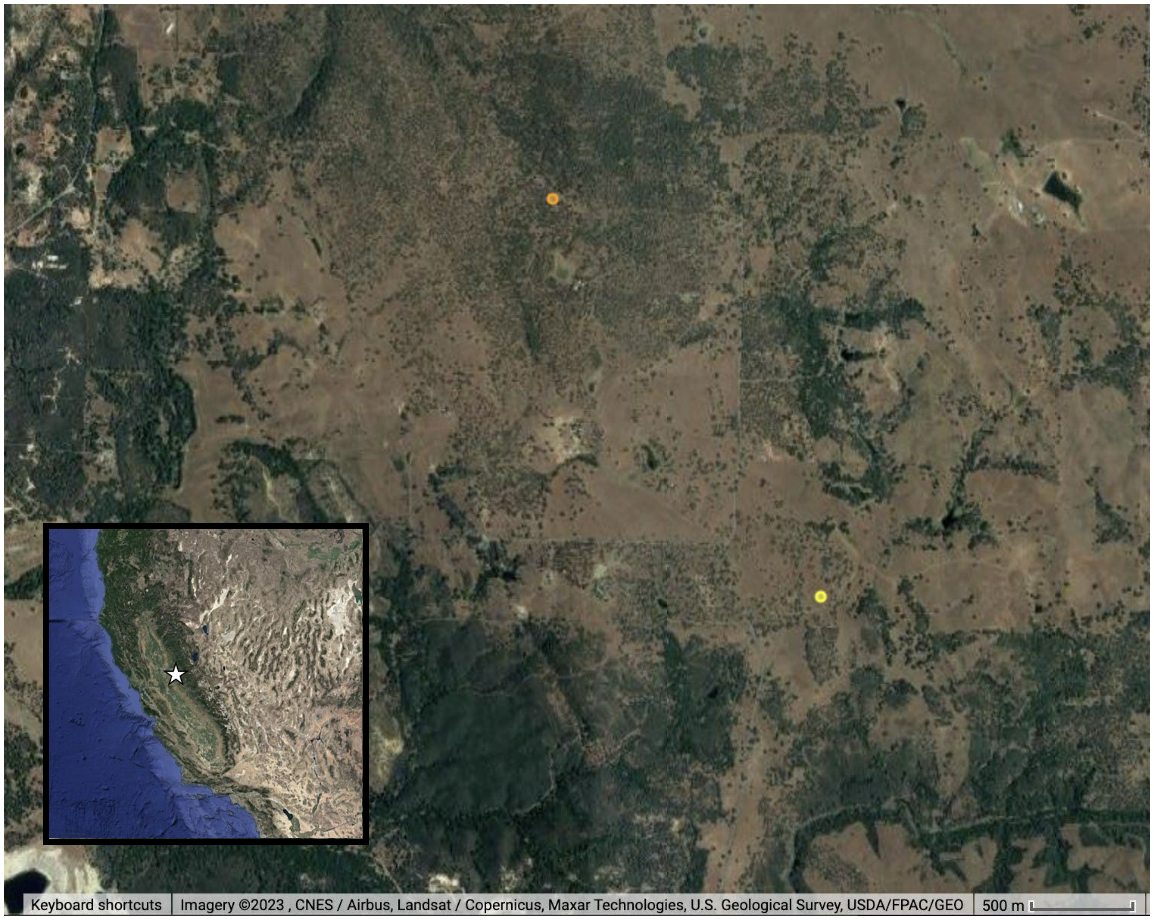

Figure 1. Geographical location of the EC towers located in Tonzi oak woodland savanna (orange) and Vaira grassland (yellow) generated by Google Earth with inset showing site location (star) within California.

Data Collection

Eddy covariance data

To obtain the eddy covariance (EC) data from Tonzi and Vaira, I downloaded the BASE product CSV files that are publicly available on the AMERIFLUX website for both ecosystem types for the study period (January 1, 2016- December 31, 2021). The BASE product is data that has been processed using the Flux-Processing Standard in order to provide standardized variables with a half-hourly or hourly temporal aggregation (https://ameriflux.lbl.gov/data/aboutdata/). Eddy covariance data comprises of information on biosphere-atmosphere feedbacks derived by measurements of temperature, water, CO_2 , and heat flux exchanges including Latent heat flux (LE), Sensible heat flux (H), Vapor Pressure Deficit (VPD), Volumetric soil water content

(SWC), and Gross Primary Production (GPP) (Baldocchi et al. 2003). These variables provide an interpretation of the net radiation balance and energy partitioning relationships within these two ecosystems when differing soil moisture conditions are present.

Satellite remote sensing data

To obtain the satellite imagery for Tonzi and Vaira, I downloaded the past 6 recent years of geospatial data (2016-2021) from the Moderate Resolution Imaging Spectroradiometer (MODIS) satellite sensor (https://modis.gsfc.nasa.gov/data/) through the A*pp*EEARS NASA Earthdata database (https://appeears.earthdatacloud.nasa.gov/) to acquire information about photosynthesis and net radiation balance for both ecosystems. This data was extracted using the point samples for the geographic coordinates of the oak woodland savanna and grassland. MOD V006 data provides insight into vegetation greenness associated with photosynthesis and vegetation productivity such as Normalized Difference Vegetation Index (NDVI) and Enhanced Vegetation Index (MOD13Q1.006, 500 m spatial and 16-day temporal resolutions); Gross Primary Production (GPP) (MOD17A2H.006, 500 m spatial and 8-day temporal resolutions); Evapotranspiration (ET) (MOD16A2GF.006, 500 m spatial and 8-day temporal resolutions); and Leaf Area Index (LAI) and fraction of Absorbed Photosynthetically Active Radiation (fAPAR) (MOD15A2H.006, 500 m spatial and 8-day temporal resolutions). These products are informative of the relationships between different vegetation indices and vegetation structure changes, which supports the eddy covariance data by using larger-scaled spectral information observed from space.

Designating wet and dry year within the study period

In order to center my analyses on the water availability in the ecosystem sites, I focused on the Water Years (WY) that starts October 1 and ends September 30 of the following year. For example, WY2017 includes October 2016 to September 2017. To categorize the wet and dry year within the study period, I ranked the precipitation (mm) levels in WY over the 20 years of available eddy covariance data. This determined how the wet and dry years within my study period compared to the overall precipitation inputs for both ecosystems on a much larger temporal scale.

Seasonal Dynamics of Energy Balance and Vegetation Productivity

Analysis using eddy covariance data

To analyze the measurements of energy balance partitioning and vegetation productivity, I used the MATLAB software to first load in the Tonzi and Vaira Ameriflux BASE products that include half-hourly observations from 2001 to 2022. To organize the variables and analyze the time series from 2016-2021 with consistent time increments, I aggregated the data into monthly and daily intervals for air temperature, precipitation, LE, H, GPP, and VPD to create new columns for plotting time series graphs. I took the daily mean of the LE, H, SWC, VPD, and air temperature measurements within each day and the daily sum of precipitation over the 6 years of data. In order to create the new GPP, I converted the units from µmol CO_2 m^{-2} s^{-1} to g C m^{-2} d^{-1} and took the daily sums of the data. I added a threshold to remove LE and H for values when GPP <=0 to focus on the daytime observations on a daily basis because when GPP values are 0, the vegetation is no longer undergoing photosynthesis. Following the data cleaning and aggregations in MATLAB, I continued my data analyses and time series visualizations by loading the edited CSV files into Python and utilized different Python libraries (Pandas, Numpy, Plotly, and Scipy) for the rest of the analyses.

GPP encompasses several different heat and energy fluxes, so it is necessary to sum the daily observations before aggregating the data to monthly means to minimize sampling errors (Baldocchi 2020). GPP is measured from the perspective of the ecosystem (positive = carbon uptake) (Baldocchi 2017). Net radiation balance describes the energy balance between the solar energy absorbed by the ecosystem and the heat energy fluxes released into the atmosphere or deposited back into the soil (R_{net}=H+LE+G+ΔS), with net radiation (Rnet), sensible heat (H), latent heat (LE), ground heat flux (G), and change in storage (ΔS). Positive value heat fluxes on the right of the equation indicate energy leaving the surface. When net radiation (R_{net}) values on the left are positive, the sum of LE and H is larger than G and ΔS.

To understand the relationship between energy balance and vegetation productivity, explaining the interdependence between latent heat and sensible heat fluxes is necessary. LE (W m^{-}) is the heat energy transferred to the atmosphere when evapotranspiration occurs. Evapotranspiration (ET) is the sum of the evaporation from vegetation or soil surfaces and water loss transpired by the plants' stomata; this process drives the water transfer between the land and the atmosphere, or the latent heat flux within a system. LE, therefore, links ecosystem water loss to the energy budget that drives evapotranspiration (Chapin and Mooney 2002). H (Wm^{-2}) is the heat energy initially transferred between the canopy and the atmosphere, which is mainly driven by the air temperature difference between the two. When surface temperatures increase due to the released heat energy from the canopy (+H), the water-holding potential of the atmosphere increases (large VPD), which drives the release of water vapor from the canopy surface and into the atmosphere (+LE) if sufficient water is available. These interdependencies between LE and H directly relate to the atmospheric vapor pressure gradient— and therefore VPD — that drives evapotranspiration (Chapin and Mooney 2002).

In order to categorize the periods of time that the Tonzi and Vaira sites are undergoing water stress, I first calculated the daytime Evaporative Fraction (EF= LE/(LE + H)) to the entire 6-year time scale. This measure is known to respond to changes in meteorological conditions, including precipitation and soil water content, in relation to energy cycling within an ecosystem. I focused on this measure when testing relationships to investigate the water and energy balance changes in relation to a wet and dry year.

To investigate the seasonal energy flux dynamics of the oak woodland and grassland over the 2016-2021 time range, I first plotted the 6-year time series for air temperature, precipitation, LE, H, EF, VPD, and GPP. This provided me with a visual understanding of the oscillating seasonal behaviors of both ecosystems and when each of these variables peaks seasonally. From the time series, I extracted information on rainfall events and the minima and maxima of these environmental and biophysical variables to give perspective on the overall changes in productivity and energy balance partitioning in a wet and dry year in a Mediterranean climate.

Additionally, I focused on the growing season (May-October) and spring (March-May) for part of my study to center the analyses around vegetation productivity and total GPP.

To assess the relationships between the environmental variables of interest, I plotted LE, H, EF, and VPD with GPP; LE, H, and VPD with SWC; and SWC and GPP to deduce if there is a linear relationship present. I used the Ordinary Least Square (OLS) regression trendline from the Plotly library to observe the R^2 values. Following this step, I performed a yearly Spearman's Rank Correlation between these pairs of variables to find the direction and strength without assuming a linear relationship. I tested the significance of these relationships with 95% and 99% confidence levels using t-testing.

To investigate the seasonal dynamics of the relationship between evapotranspiration and vegetation productivity in a wet and dry year, I plotted the monthly aggregated LE and GPP with colorized points representing each month with OLS trendlines for the two years to visualize the linearity of the relationship with R^2 values and points where both variables peak during specific months of the year for both the oak woodland savanna and grassland. By processing and analyzing EC data to explain energy balance changes in relation to soil moisture availability, I was able to distinguish the different relationships and compare their strength and directionality between wet and dry years and ecosystem types.

Seasonal Dynamics of Soil Moisture and Photosynthesis

Analysis using eddy covariance data

To investigate the seasonal soil moisture dynamics of the oak woodland and grassland over the 2016-2021 period, I first plotted the 6-year time series for SWC and GPP. I extracted information during the wet and dry year to compare the months when GPP peaks and the range SWC (%) specific to the growing season.

To assess the relationships between SWC and GPP, I performed a monthly Spearman's Rank Correlation and tested the significance of those correlations using a t-test. With the months that showed the strongest significant correlation, I visualized a plot with SWC and GPP to understand the coupling between the two on a daily scale. I expect that the oak woodland savanna will overall have a larger range of SWC in comparison to the grassland.

Analysis using remote sensing data

To analyze the soil moisture and photosynthesis observations, I loaded the 5 different data product tables into the Jupyter Notebook. To organize the variables and analyze the time series from 2016-2021 with consistent time increments, I first filtered the specific variables I wanted to analyze and performed initial unit conversions for dimensional analysis (GPP, NDVI, LAI, fAPAR, and ET). For ET and GPP, I divided by 8 as the initial observations done by MODIS were at a per 8-day scale.

Radiative properties are extremely important in ecological analyses, especially when drawing conclusions about GPP levels. The Normalized Difference Vegetation Index (NDVI = (NIR - red)/(NIR + red)) is a vegetation index that uses the near-infrared (NIR) and red bands to detect the magnitude of vegetation greenness, yet it is well documented that NDVI will saturate at high LAI values and can be affected by atmospheric conditions (Gamon et al. 1995). Due to this, I also calculated the Visible Atmospherically Resistant Index (VARI), which is sensitive to changes in green vegetation fraction with atmospheric corrections. VARI is calculated using the red, green, and blue reflectance bands from MODIS:

$$(R_{green} - R_{red}) / (R_{green} + R_{red} - R_{blue})$$

I chose to use this index as it was found to be most correlated to soil moisture in an oak woodland savanna and grassland (Liu et al. 2011)

The most used approach to modeling GPP is using the light use efficiency (LUE) model which combines the potential of converting fAPAR to GPP, GPP = LUE x fAPAR x PAR, with PAR as photosynthetically active radiation, measuring the efficiency of absorbed energy to the amount of carbon fixed by an ecosystem (Croft et al. 2015, Monteith 1972). The way in which light is reflected back to satellite sensors is dependent on the type of vegetation structure present which was the motivation to analyze LAI. Oak woodland savannas are considered rougher, whereas grasslands are smoother. Ecosystem differences in GPP are determined mainly by LAI and the growing seasons, followed by environmental controls (water, energy, temperature) over photosynthesis (Chapin and Mooney 2002). Including fAPAR and LAI in my analyses provides a well-rounded interpretation of the vegetation productivity of both ecosystems as they are both proxy measures to GPP.

To create a smoothed time series to an everyday scale, I linearly interpolated my variables of interest using the time parameter in the "interpolate" Python function to visualize the seasonal oscillations in the study period. Since satellites have a lower temporal resolution compared to eddy covariance data, I wanted the 8-day observation variables to be plotted at the same temporal resolution for the initial seasonal dynamics visualizations over the 6 years of data.

To assess the relationships between the environmental variables of interest, I plotted NDVI, LAI, fAPAR, and ET with GPP; LAI, fAPAR, and GPP with VARI; and LAI, GPP, and VARI with ET to deduce if there is a linear relationship present. I used the Ordinary Least Square (OLS) regression trendline from the Plotly library to observe the R^2 values. Following this step, I performed a yearly Spearman's Rank Correlation between these pairs of variables to find the direction and strength without assuming a linear relationship. I tested the significance of these relationships with 95% and 99% confidence levels using t-testing. By processing and analyzing MODIS data to explain vegetation productivity changes in relation to soil moisture availability, I was able to distinguish the different relationships and compare their strength and directionality between wet and dry years and ecosystem types.

Vegetation Productivity Response Timing in a Wet and Dry Year

Analysis using eddy covariance data

To investigate the lag of SWC over the calendar year study period, I first performed cross-correlation analyses during the spring (March-May), which assesses the highest correlation between SWC and GPP when SWC is lagged a certain amount of days. The dry-down period in the Mediterranean climate typically occurs in late spring, which is why I focused on the cross-correlation for that period. Once I found the lag days for each year for both ecosystems, I shifted the SWC columns to that lag day. I then performed a Spearman's Rank correlation between SWC and lagged SWC with GPP in the spring to assess whether the lag improved the relationships between soil moisture and vegetation productivity.

To investigate the timing between GPP and SWC in a wet and dry year, I first performed a Singular Spectral Analysis (SSA) using the Pyts library on WY2017 and WY2020, which helps classify and analyze time series data. SSA is a nonparametric spectral estimation method that allows smoothing out the unnecessary noise, assisting in pinpointing on what day GPP and SWC decline in late spring. To pinpoint when this changes from increasing to decreasing value, I took the derivative of GPP and SWC. I designated this change by finding the last peak in both time series showing the period of declining GPP and soil moisture dry-down later in spring. I expect GPP will decline earlier in the dry years than the wet where there is a lack of soil moisture availability, with the oak woodland savanna being more robust to soil moisture changes and GPP timing differences in the dry year compared to the grassland.

RESULTS

Climate

I visualized the Mediterranean climate for the 2016-2021 period through a daily aggregated time series of air temperature and precipitation (Figure 2). The annual precipitation and mean annual volumetric soil water content over the study period in water years (October 1, 2017 - September 31, 2021) are shown in Table 1. The wettest year is designated as 2017 and the driest year is 2021.

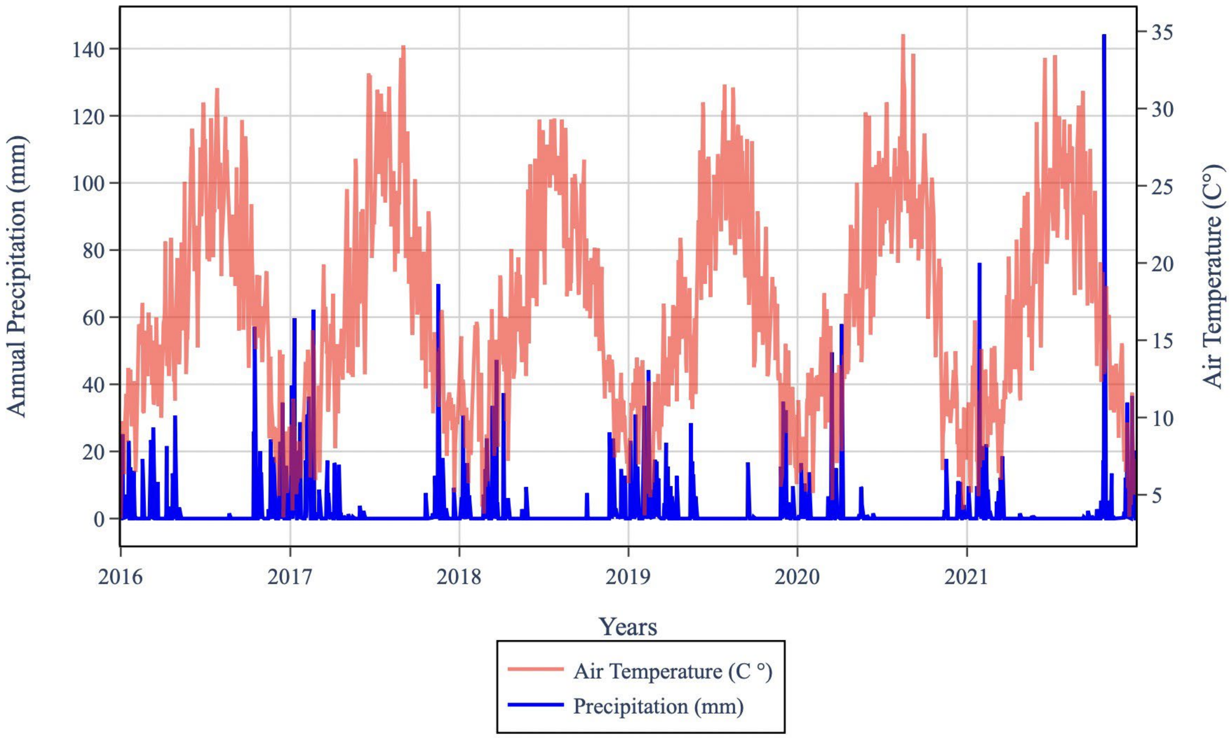

Figure 2. Daily aggregated time series of Mediterranean climate over the 2016-2021 period in the oak savanna grassland (small temperature differences to grassland). Air temperature (red) consistently peaks in the summer for both ecosystem types. Precipitation levels (blue) show that rainfall events mostly happen in the winter.

During WY 2021, the driest year of the study in the oak woodland, I found smaller ranges in air temperatures, from a minimum of 4 ℃ in the winter and a maximum of 18.5℃ in early spring, to a maximum of 33.5 ℃ by early summer. During the same year, the grassland showed a similar range in air temperatures, from a minimum of 3.3℃ in the winter and a maximum of 23.9 ℃ in early spring to 33.2 ℃ by early summer. Comparing the seasonal temperature fluctuations between 2017 and 2021, the grassland showed to have the largest change in the air temperature range in the early spring (March-May) from 11.8 ℃ in the wet year to 18.1℃ in the dry year.

In the wet year, I found that there were distinct rainfall events on October 16, 2016, with 57.15mm, January 10, 2017, with 59.7 mm, and February 20, 2017, with 62.23 mm. The first rainfall event triggered an increase of SWC from 4% to 39.6% in the oak savanna and an increase of 1.5% to 28.9% SWC in the grassland. In the dry year, there was an extreme rainfall event on January 28, 2021, with 76.2 mm which was 22% of the total rainfall that year. That first rainfall event triggered the SWC in the oak woodland to increase from 12.7% to 50.1% and

15.89% to 35.41% in the grassland. The WY2021 ends prior to the extreme rainfall event that occurred on October 24, 2021, with 144.28 mm, where there was a 49.7% and 40.27% difference in SWC in the oak savanna and grassland respectively. From a calendar year perspective, 2020 is the driest year with an annual precipitation of 350.3 mm and 2021 became the third driest with 700 mm.

Table 1. Annual sum precipitation and mean annual volumetric soil water content for the California water year (October 1- September 30).

Water Year	Annual Precipitation (mm)	Oak Woodland Mean Annual SWC (%)	Grassland Mean Annual SWC (%)
2017	1032.50	24.31	19.66
2018	580.40	18.62	16.13
2019	846.07	21.51	20.30
2020	434.60	16.24	15.80
2021	348.74	14.23	10.38

Seasonal Dynamics of Energy Balance and Vegetation Productivity

In an oak woodland savanna

The study period time series of latent heat (LE) and sensible heat (H) in the oak woodland savanna is shown in **Figure 3**.

The highest peak of LE had a monthly mean value of 151.23 W $m^{-2}\, d^{-1}$ in April 2016, and the lowest peak with a mean value of 118.24 W $m^{-2}\, d^{-1}$ during April 2021. The highest peak of H had a monthly mean value of 237.17 W $m^{-2}\, d^{-1}$ during July 2020, and the lowest peak with a mean value of 209.23 W $m^{-2}\, d^{-1}$ during August 2017. Out of the entire study period, the highest daily integrated LE value reached 216.53 W $m^{-2}\, d^{-1}$ in May 2017 and the lowest reached -6.81 W $m^{-2}\, d^{-1}$ in October 2020. The highest LE value is the maximum for the 2017 water year, and the lowest LE value is the minimum for the 2021 water year. Out of the entire study period, the highest daily integrated H value reached 308.01 W $m^{-2}\, d^{-1}$ in May

2017, and the lowest reached -59.30 W $m^{-2}\ d^{-1}$ in March 2020. The highest H value is the maximum of the 2017 water year, while the lowest H value is not the minimum of the 2021 water year, being -11.57 W $m^{-2}\ d^{-1}$.

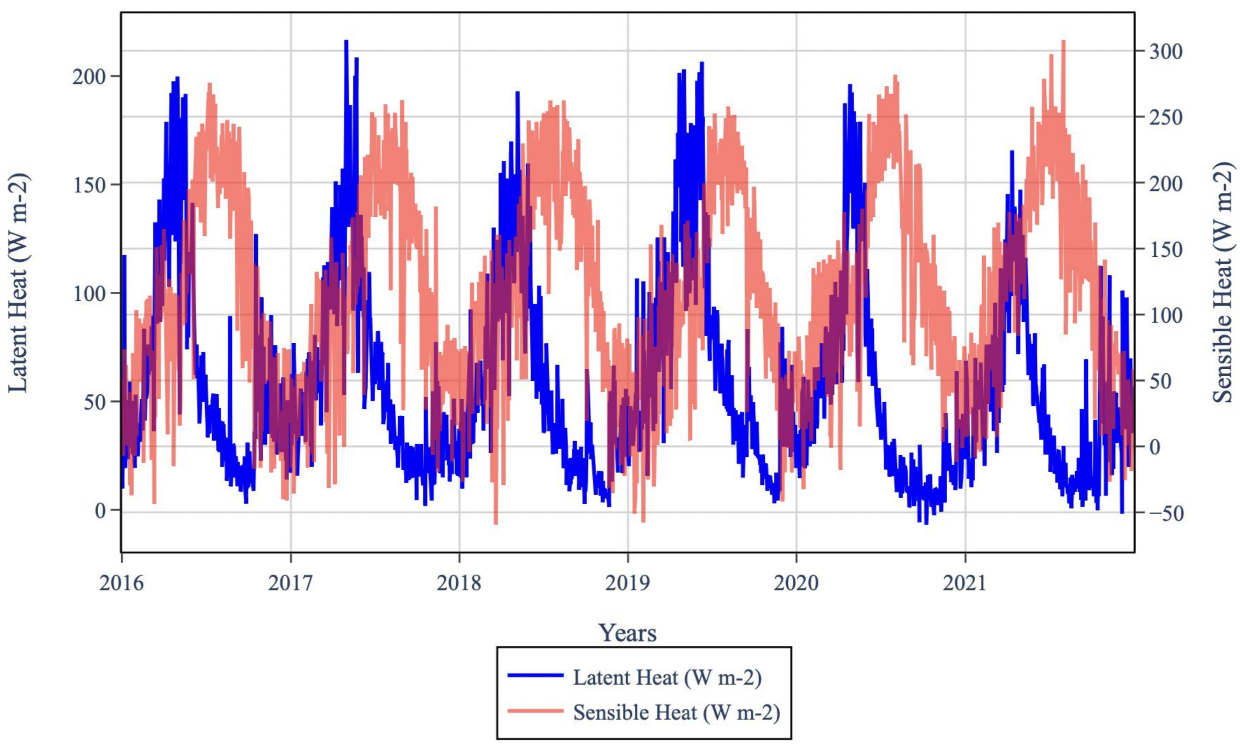

Figure 3. Seasonal oscillations of daily-integrated daytime latent heat (blue) and sensible heat (red) in the oak woodland savanna. Latent heat tends to peak during the later spring months (April-May). Sensible heat tends to peak during the summer months (June-August).

The relationships between soil moisture and different biophysical and environmental variables are shown to be overall consistent in the oak woodland savanna. The coefficient results from performing the Spearman's Rank correlation over the water year study period are shown in Table 2. LE and GPP have a linear relationship and a consistently strong positive correlation over the study period. H and GPP do not have a linear relationship and a weak correlation in 2018, 2019, and 2021. EF and GPP do not have a linear relationship, but do present overall strong positive rank correlation coefficients, with the dry year having the smallest value (Figure **A1**). I did not find significant values for VPD and GPP. SWC and LE do not have a linear relationship, with strong positive coefficients in the drier years of 2020 and 2021. I observed a seasonal trend between SWC and LE where both hit a minimum in September-November, June, and August. SWC and H have an overall linear relationship and a negative rank correlation, the strongest being in the wet year of 2017. SWC and EF have an overall strong positive correlation over the study period. SWC and GPP do not have a linear relationship and show hysteresis and an overall weak positive rank correlation. SWC and VPD have a linear relationship and an overall strong negative correlation throughout the study period.

Table 2. Spearman's Rank correlation coefficients of relationships between eddy covariance environmental variables of interest in the oak woodland savanna. All relationships are significant at the 99% level except for the ones labeled as * at the 95% level and as n.s. for not significant ($p > 0.05$)

Water years	**LE vs GPP**	**H vs GPP**	**EF vs GPP**	**VPD vs GPP n.s.**	**SWC vs LE**	**SWC vs H**	**SWC vs EF**	**SWC vs GPP**	**SWC vs VPD**
2017	0.733	0.0473 n.s.	0.386	-0.0222	0.273	-0.736	0.734	0.270	-0.791
2018	0.797	0.127*	0.486	-0.101	0.579	-0.535	0.777	0.516	-0.653
2019	0.786	0.280	0.338	0.0875	0.469	-0.572	0.797	0.234	-0.709
2020	0.801	0.0934 n.s.	0.521	-0.0452	0.700	-0.412	0.779	0.563	-0.518
2021	0.716	0.367	0.420	-0.0216	0.696	-0.408	0.812	0.377	-0.602

In the oak woodland, I found that there is a strong positive relationship between the energy balance variable latent heat and vegetation productivity for both the wet and dry year (Figure 4). The Ordinary Least Square regression trendline generated an R^2 value of 0.88 for both years. LE and GPP both peak during May in the wet year and April in the dry year. See the Appendix for H and GPP over the wet year and dry year (Figure A3).

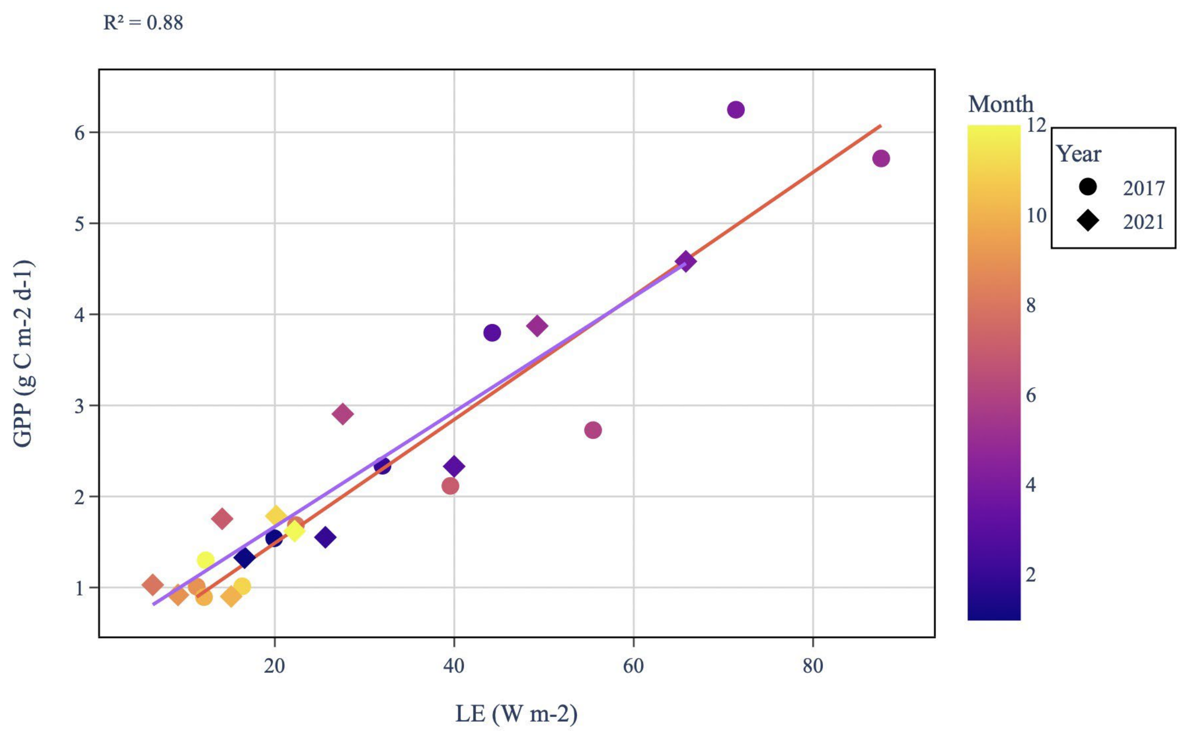

Figure 4. Oak woodland seasonal dynamics of the relationship between monthly aggregated latent heat (LE) and gross primary production (GPP) in the wet (2017) and dry (2021) years. The generated orange (2017) [y = 0.0678922x + 0.129489] and purple (2021) [y = 0.0630934x + 0.406853] trendlines show the linear relationship between LE and GPP

In a grassland

The study period time series of latent heat (LE) and sensible heat (H) in the grassland is shown in Figure 5.

The highest peak of LE had a monthly mean value of 159.85 W m^{-2} d^{-1} during April 2016, and the lowest peak with a mean value of 119.74 W m^{-2} d^{-1} during April 2021. The highest peak of H had a monthly mean value of 152.85 W m^{-2} d^{-1} during July 2020, and lowest peak with a mean value of 102.62 W m^{-2} d^{-1} during May 2016. Out of the entire study period, the highest daily integrated LE value reached 214.75 W m^{-2} d^{-1} in May 2017 and the lowest reached -9.10 W m^{-2} d^{-1} in September 2021. The highest LE value is the maximum of the 2017 water year and the lowest LE value is also the minimum of the 2021 water year. Out of the entire study period, the highest daily integrated H value reached 220.17 W m^{-2} d^{-1} in

June 2019, and the lowest reached -57.12 W $m^{-2}\ d^{-1}$ in January 2019. The highest H value is not the maximum of the 2017 water year, being 185.50 W $m^{-2}\ d^{-1}$ while the lowest H value is not the minimum of the 2021 water year, being -33.68 W $m^{-2}\ d^{-1}$.

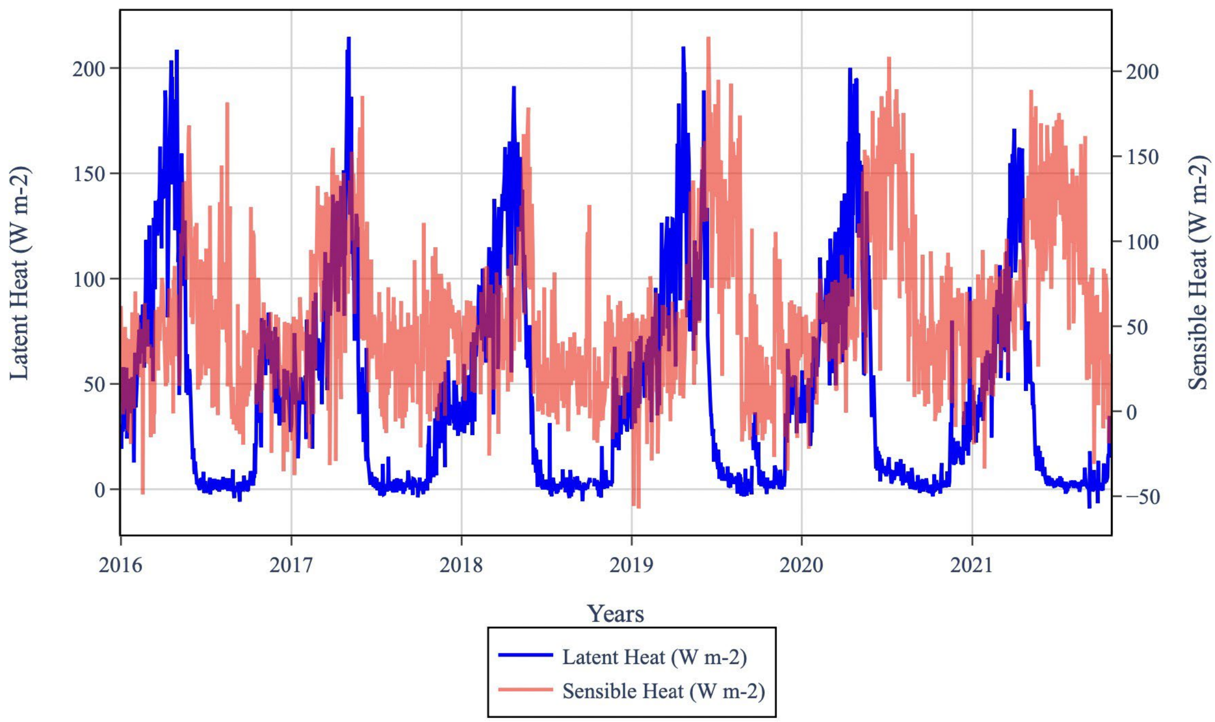

Figure 5. Seasonal oscillations of daily-integrated daytime latent heat (blue) and sensible heat (red) in the grassland. Latent heat consistently peaks in April. Sensible heat peaks in May except for the years 2019 and 2020 peaking in June and July respectively.

The relationships between soil moisture and different biophysical and environmental variables are shown to be overall consistent in the grassland. The coefficient results from performing the Spearman's Rank correlation over the water year study period are shown in Table 3. LE and GPP have a linear relationship and a consistently strong positive correlation over the study period. H and GPP do not have a linear relationship and overall weak positive correlation with the exception of 2018. EF and GPP do not have a linear relationship, but do present overall strong positive rank correlation coefficients, with the wet year having the smallest value (Figure A2). VPD and GPP do not have a linear relationship but do present overall negative rank correlations. SWC and LE do not have a linear relationship with strong positive rank coefficient values, with the strongest being in the dry year. I observed a seasonal trend between SWC and LE where both hit a minimum in September-November and June-August. SWC and H have an overall linear relationship and weak negative rank correlations in 2018 and 2020. SWC and EF have an overall strong positive correlation over the study period. SWC and GPP do not have a linear relationship and show hysteresis and an overall strong positive rank correlation. SWC and VPD have a linear relationship and an overall strong negative correlation throughout the study period, the strongest correlation being in the wet year and the weakest being in the dry year.

Table 3. Spearman's Rank correlation coefficients of relationships between eddy covariance environmental variables of interest in the grassland. All relationships are significant at the 99% level except for the ones labeled as* at the 95% level and as n.s. for not significant at any level.

Water years	LE vs GPP	H vs GPP	EF vs GPP	VPD vs GPP	SWC vs LE	SWC vs H	SWC vs EF	SWC vs GPP	SWC vs VPD
2017	0.889	0.0467	0.640	-0.577	0.646	0.0927 n.s.	0.662	0.660	-0.853
2018	0.901	0.516	0.754	-0.613	0.729	0.337	0.724	0.742	-0.806
2019	0.885	0.0995 n.s.	0.700	-0.566	0.674	-0.0183 n.s.	0.654	0.692	-0.663
2020	0.905	0.131*	0.733	-0.567	0.614	-0.359	0.719	0.627	-0.841
2021	0.847	0.0352 n.s.	0.753	-0.5424	0.819	-0.0949 n.s.	0.767	0.738	-0.636

I found that there is a strong positive relationship between the energy balance variable latent heat and vegetation productivity for both the wet and dry year (Figure 6). The Ordinary Least Square trendline generated an R^2 value of 0.93 for the wet year and 0.96 for the dry year. LE and GPP both peak during April in 2017 and 2021. Both variables peak at much higher values in May of the wet year in comparison to May of the dry year. See Appendix for H and GPP over the wet year and dry year (Figure A4).

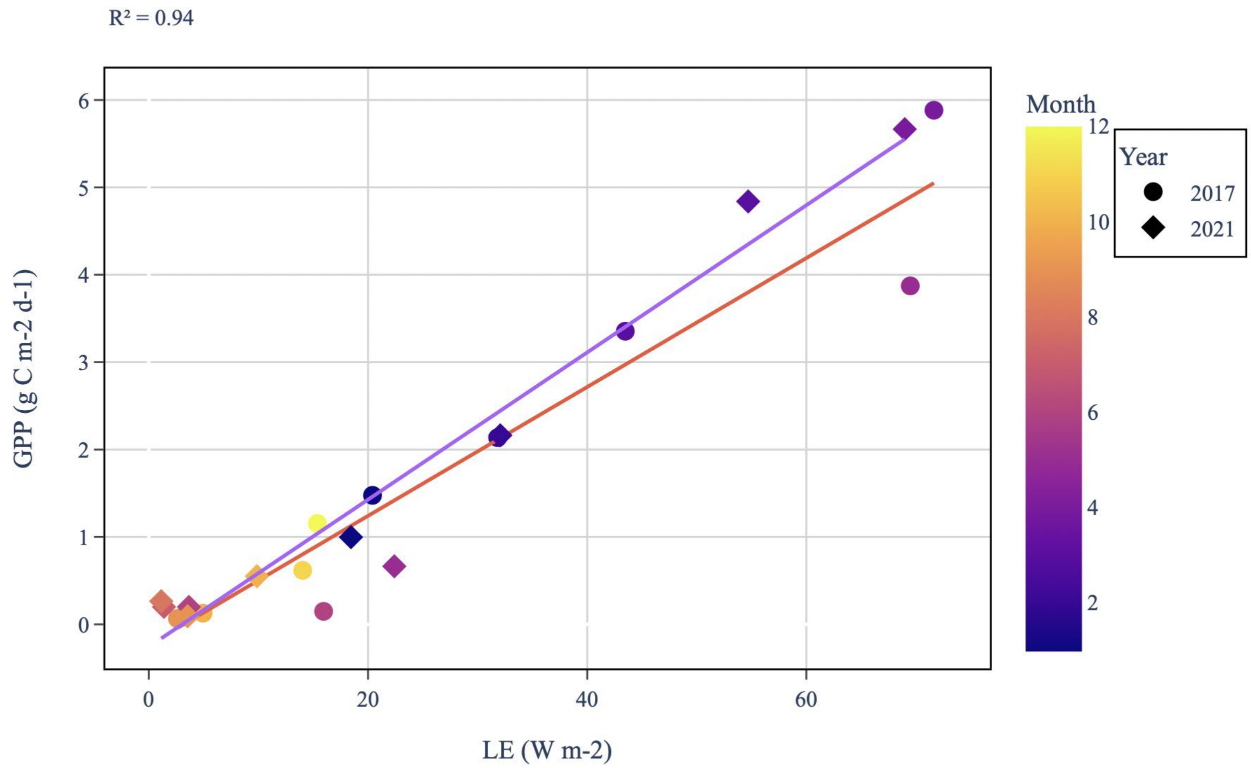

Figure 6. Grassland seasonal dynamics of the relationship between monthly aggregated latent heat (LE) and gross primary production (GPP) in the wet (2017) and dry (2021) years. The generated orange (2017) [y = 0.0737434x + -0.233703] and purple (2021) [y = 0.084201x + -0.256518] trendlines show the strong positive linear relationship between LE and GPP.

Seasonal Dynamics of Soil Moisture and Photosynthesis

In an oak woodland savanna

The study period time series of soil moisture (SWC) and daily assimilated photosynthesis (GPP) in the oak woodland savanna is shown in Figure 7. In the wet and dry year, GPP reached a maximum of 11.42 g C m^{-2} d^{-1} and 6.13 g C m^{-2} d^{-1} respectively. GPP peaks in April for the drier years (2018, 2020, 2021) and peaks in May for the wetter years (2017, 2019). In the wet year, I found that the total amount of GPP assimilated over the growing season (May-October) was 434.76 g C m^{-2} d^{-1} and SWC ranged from 3.89% to 52.91%. In the dry year, the total amount of GPP during the growing season reached 348.96 g C $m^{-2}d^{-1}$and SWC ranged from 4.28% to 50.12%.

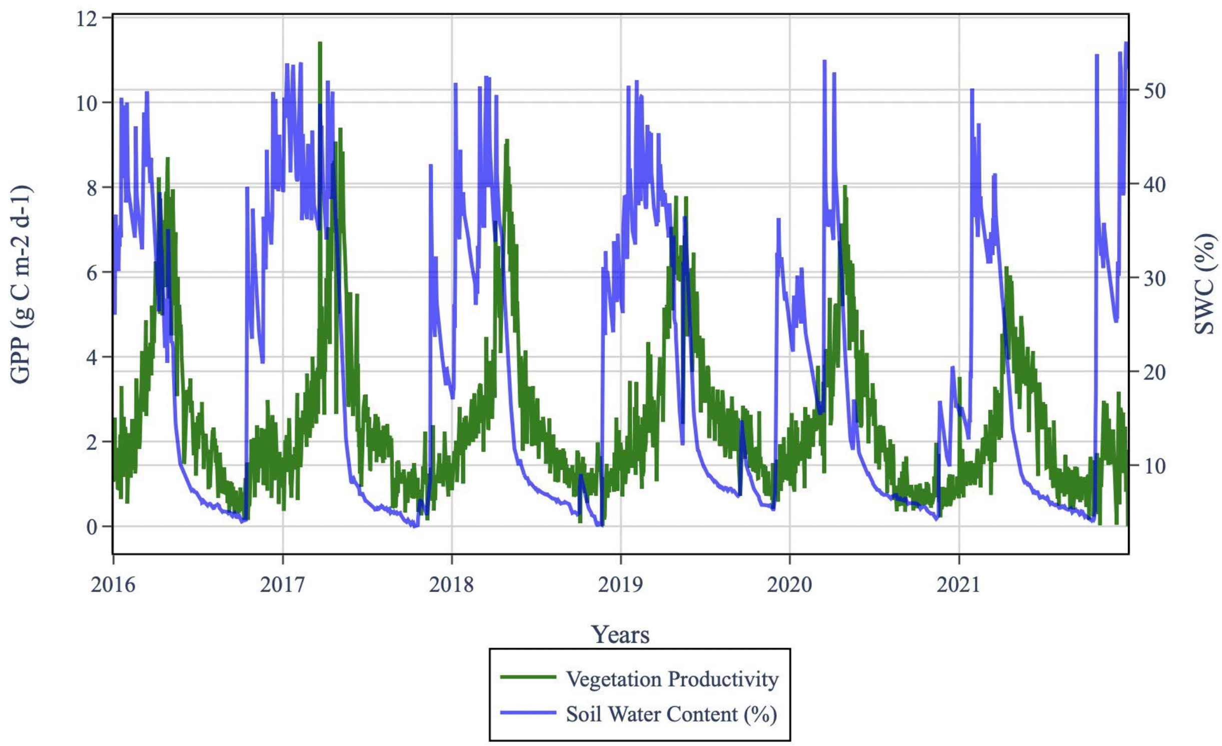

Figure 7. Seasonal oscillations of daily-integrated photosynthesis (GPP, green) and volumetric soil water content (blue) in the oak woodland via eddy covariance.

During the wet year in the oak woodland, I found that SWC and GPP had the strongest positive relationship in May (Figure A5). The Spearman's Rank correlation coefficient had a value of 0.726 with a $p<0.05$ significance level. Soil moisture levels drop from 30% on Day 1 to 5% on Day 30 (Figure 8).

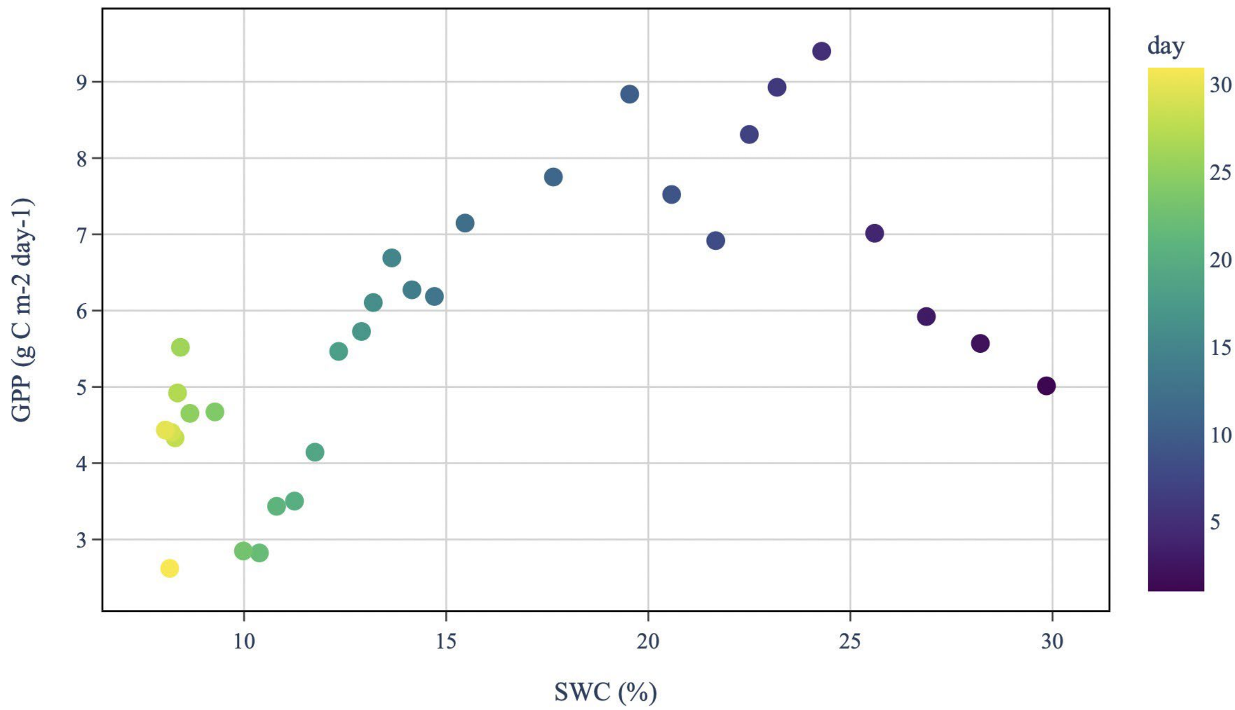

Figure 8. Oak woodland seasonal dynamics of the relationship between daily aggregated volumetric soil water content (SWC) and photosynthesis (GPP) in May 2017. SWC and GPP are most coupled in the dry-down period that occurs in late spring.

The relationships between the MODIS products and vegetation indices show to be consistent over the oak woodland savanna, yet there was no visible difference between wet and dry years. The coefficient results from performing the Spearman's Rank correlation over the water year study period are shown in Table 4. GPP and NDVI did have a significant relationship across the study period. GPP and LAI have a linear relationship and overall strong positive rank correlation. GPP and fAPAR have a linear relationship and overall strong positive rank correlation. VARI and LAI have a weak linear relationship and weak positive rank correlation (Figure A7). VARI and GPP have a weak linear relationship and weaker positive rank correlations in 2018, 2020, and 2021. VARI and fAPAR have a linear relationship and strong positive rank correlations (Figure A11). ET and GPP have a positive linear relationship and strong positive rank correlation (Figure A13). ET and LAI overall have a positive linear relationship and strong positive rank correlation. Finally, ET and VARI overall have a linear relationship and strong positive rank correlation (Figure A9).

Table 4. Spearman's Rank correlation coefficients of relationships between MODIS products and vegetation indices in the oak woodland savanna. All relationships are significant at the 99% level except for the ones labeled as* at the 95% level and as n.s. for not significant at any level.

Water years	**GPP vs NDVI n.s.**	**GPP vs LAI**	**GPP vs fAPAR**	**VARI vs LAI**	**VARI vs GPP**	**VARI vs fAPAR**	**ET vs GPP**	**ET vs LAI**	**ET vs VARI**
2017	0.0422	0.674	0.596	0.384	0.197 n.s.	0.672	0.799	0.650	0.608
2018	0.237	0.672	0.667	0.425	0.339*	0.702	0.735	0.546	0.583
2019	0.146	0.861	0.641	0.376	0.275 n.s.	0.675	0.704	0.736	0.733
2020	0.149	0.829	0.777	0.428	0.428	0.692	0.798	0.699	0.782
2021	0.132	0.803	0.819	0.442	0.503	0.585	0.766	0.686	0.723

In a grassland

The study period time series of soil moisture (SWC) and daily assimilated photosynthesis (GPP) in the grassland is shown in Figure 9. In the wet and dry year, GPP reached a maximum of 8.46 g C $m^{-2}d^{-1}$ and 8.20 g C $m^{-2}d^{-1}$ respectively. GPP peaks in April for all years with the exception peaking in May for the wet year. In the wet year, I found that the total amount of GPP assimilated over the growing season (May-October) was 135.10 g C, $m^{-2}d^{-1}$ and SWC ranged from 1.40% to 52.94%. In the dry year, the total amount of GPP during the growing season reached 57.48 g C $m^{-2}d^{-1}$and SWC ranged from 1.05% to 35.68%.

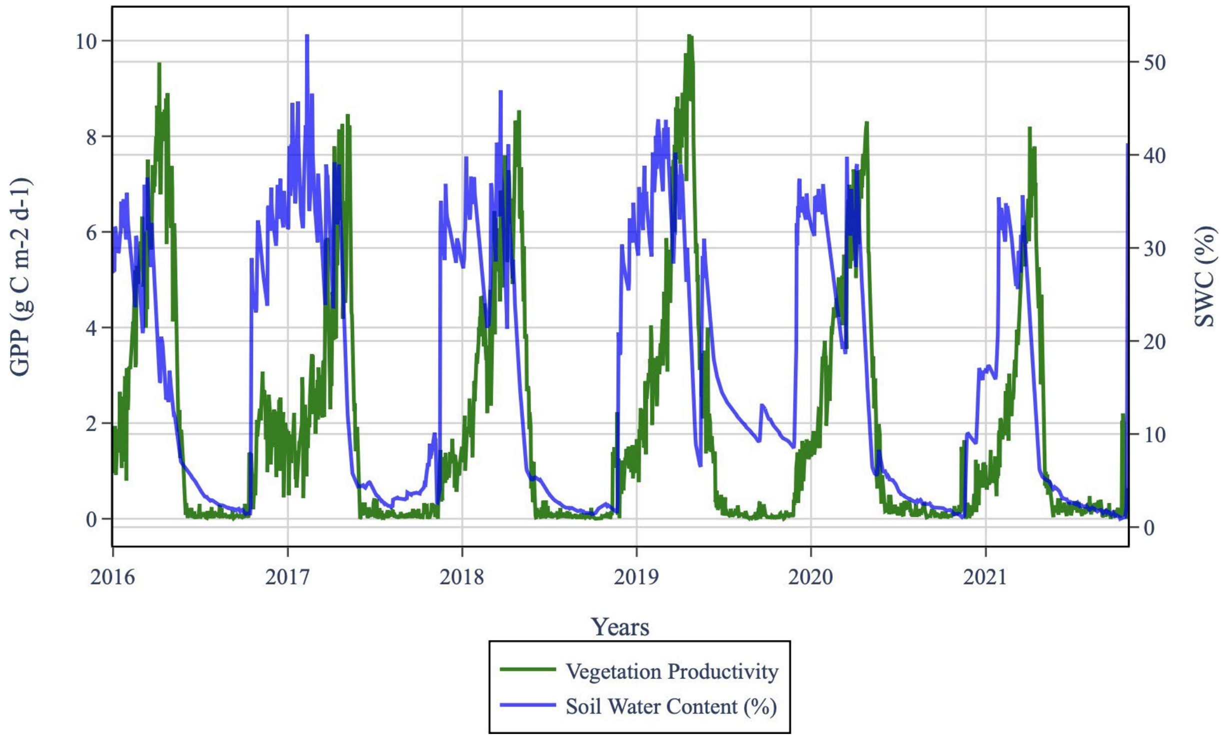

Figure 9. **Seasonal oscillations of daily-integrated photosynthesis (green) and volumetric soil water content (blue) in the grassland via eddy covariance.**

During the wet and dry year in the grassland, I found that SWC and GPP had the strongest positive relationship in May (Figure A6). The Spearman's Rank correlation coefficient values in May of the wet and dry year were 0.897 and 0.91 respectively with a $p<0.05$ significance level (Figure 10, 11). I found that there was also a strong relationship between SWC and GPP in April, with the wet and dry year values being 0.42 and 0.79 respectively at a $p <0.05$ significance level. Soil moisture levels in May 2017 dropped from 20% on Day 1 to 3% on Day 31. In May 2021, soil moisture levels dropped from 5% on Day 1 to 4% on Day 22.

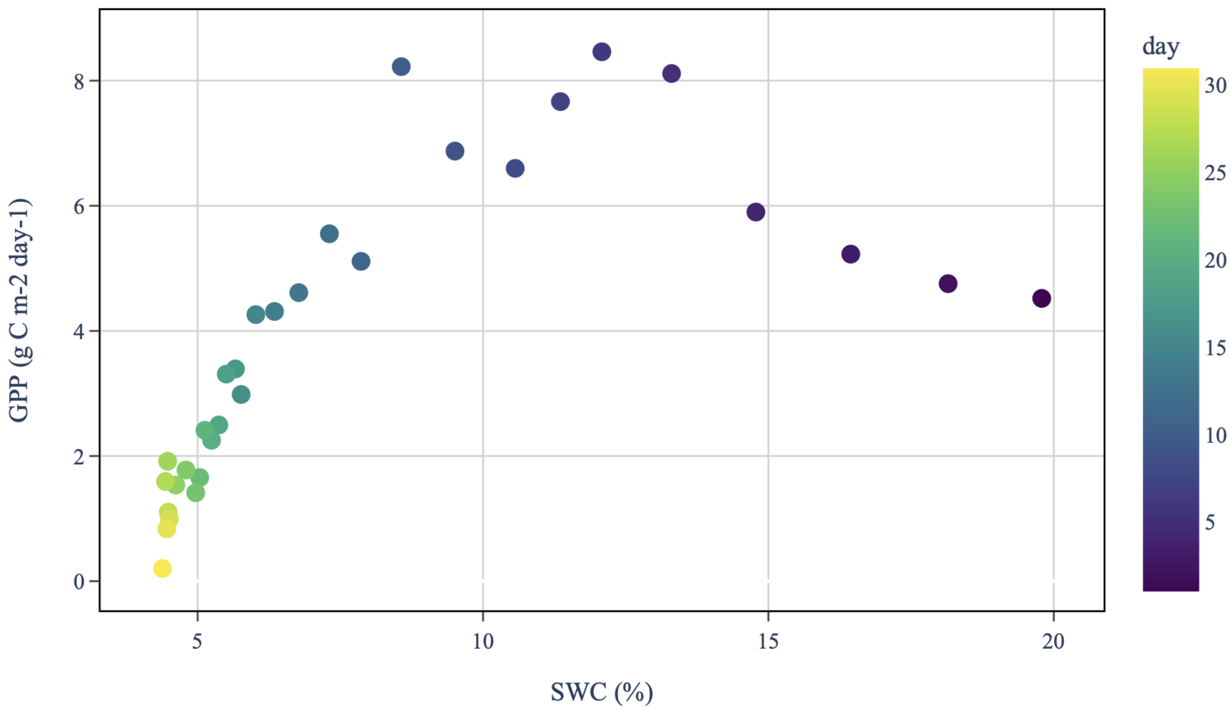

Figure 10. Grassland seasonal dynamics of the relationship between daily aggregated volumetric soil water content (SWC) and photosynthesis (GPP) in May 2017.

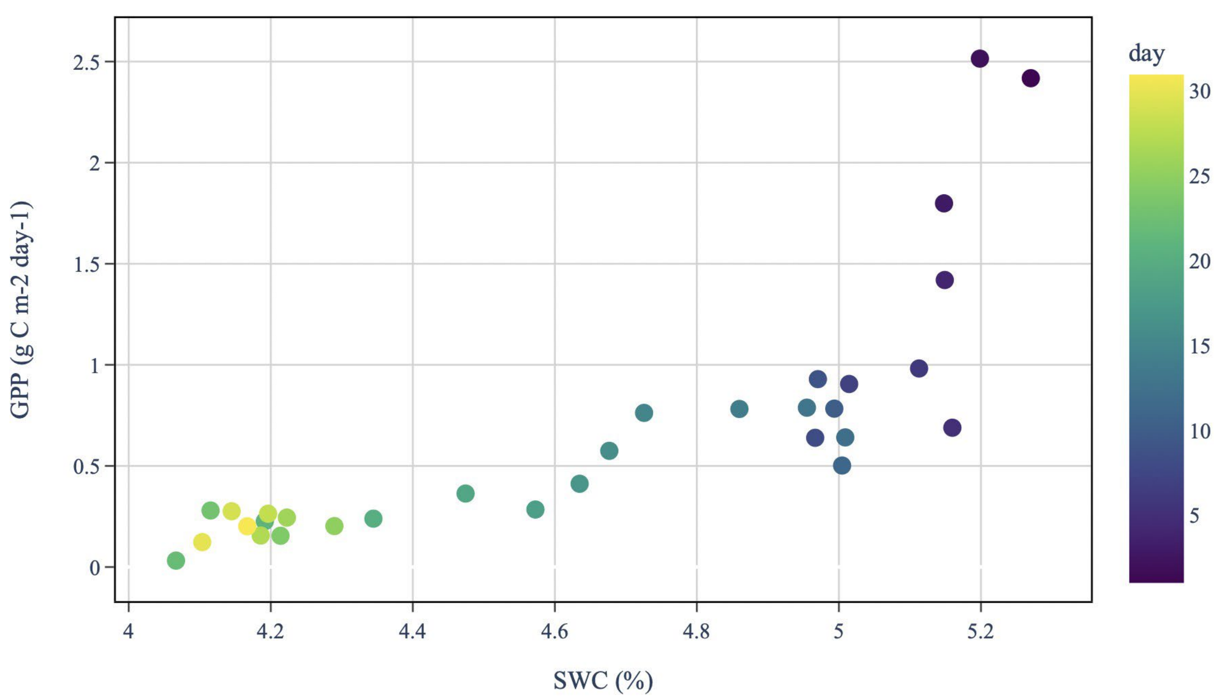

Figure 11. Grassland seasonal dynamics of the relationship between daily aggregated volumetric soil water content (SWC) and photosynthesis (GPP) in May 2021. The grasses appear to have gone through the dry-down period earlier in the dry year. Note that these are much smaller axes in both GPP and SWC than in the previous plot.

The relationships between the MODIS products and vegetation indices show to be consistent over the grassland. The coefficient results from performing the Spearman's Rank correlation over the water year study period are shown in Table 5. GPP and NDVI did not have a significant relationship across the study period. GPP and LAI have a linear relationship and overall strong positive rank correlation (Figure A8). GPP and fAPAR have a linear relationship and overall strong positive rank correlation, strongest correlation in the dry year. VARI and LAI have a weak linear relationship and a strong positive rank correlation. VARI and GPP have a weak linear relationship and the strongest positive correlation in the dry year. VARI and fAPAR have a linear relationship and strong positive rank correlations (Figure A12). ET and GPP have a positive linear relationship and strong positive rank correlation (Figure A14). ET and LAI overall have a positive linear relationship and strong positive rank correlation, with the strongest correlation in the wet year. ET and VARI overall have a linear relationship and strong positive rank correlation (Figure A10).

Table 5. Spearman's Rank correlation coefficients of relationships between MODIS products and vegetation indices in the grassland. All relationships are significant at the 99% level except for the ones labeled as * at the 95% level and as n.s. for not significant at any level.

Water years	**GPP vs NDVI n.s.**	**GPP vs LAI**	**GPP vs fAPAR**	**VARI vs LAI**	**VARI vs GPP**	**VARI vs fAPAR**	**ET vs GPP**	**ET vs LAI**	**ET vs VARI**
2017	0.0829	0.641	0.575	0.773	0.359*	0.847	0.802	0.743	0.730
2018	0.212	0.761	0.605	0.570	0.432	0.799	0.789	0.672	0.759
2019	0.159	0.766	0.590	0.654	0.433	0.799	0.722	0.7631	0.768
2020	0.182	0.798	0.675	0.702	0.589	0.815	0.777	0.757	0.808
2021	0.222	0.768	0.777	0.450	0.528	0.800	0.821	0.694	0.764

Vegetation Productivity Response Timing in a Wet and Dry Year

In an oak woodland savanna

During the spring, I found from the cross-correlation analysis that soil moisture can lag up to 17 days in the wet year and 28 days in the dry year (Table 6). The Spearman's Rank correlation coefficients between SWC and GPP all became stronger and more significant once I applied the lag. There is an overall strong positive correlation between lagged SWC and GPP except for a strong negative correlation in 2019. The drier years provided the strongest correlations between lagged SWC and GPP.

Table 6. Cross-correlation results and Spearman's Rank correlation coefficients between soil moisture and lagged soil moisture with vegetation productivity. All relationships are significant at the 99% level except for the ones labeled as n.s.

Spring (March-May)	Lag days	SWC vs GPP	Lagged SWC vs GPP
2016	16	-0.335	0.432
2017	17	-0.005 n.s.	0.602
2018	21	-0.453	0.530
2019	0	-0.669	-0.669
2020	20	0.0121 n.s.	0.764
2021	28	-0.521	0.760

During late spring, I found that the GPP response timing between the wet and dry year did not differ significantly. In the wet year, GPP dropped on May 4 and SWC dropped on April 6 (Figure 12). In the dry year, GPP dropped on April 3 and SWC dropped on March 4 (Figure 13).

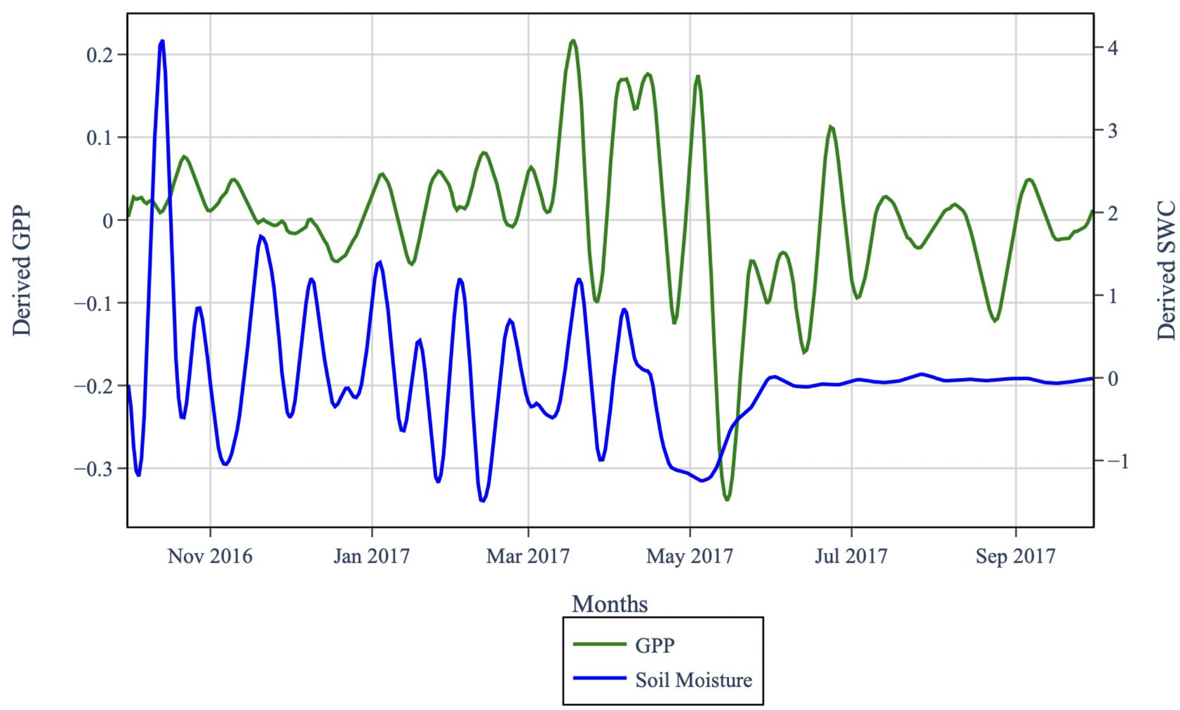

Figure 12. Smoothed time series using SSA over the wet year (WY2017) showing the dry-down timing of derived vegetation productivity (green) and derived soil moisture (blue) in an oak woodland savanna. The dry-down period for GPP dropped in May and lasted 11 days.

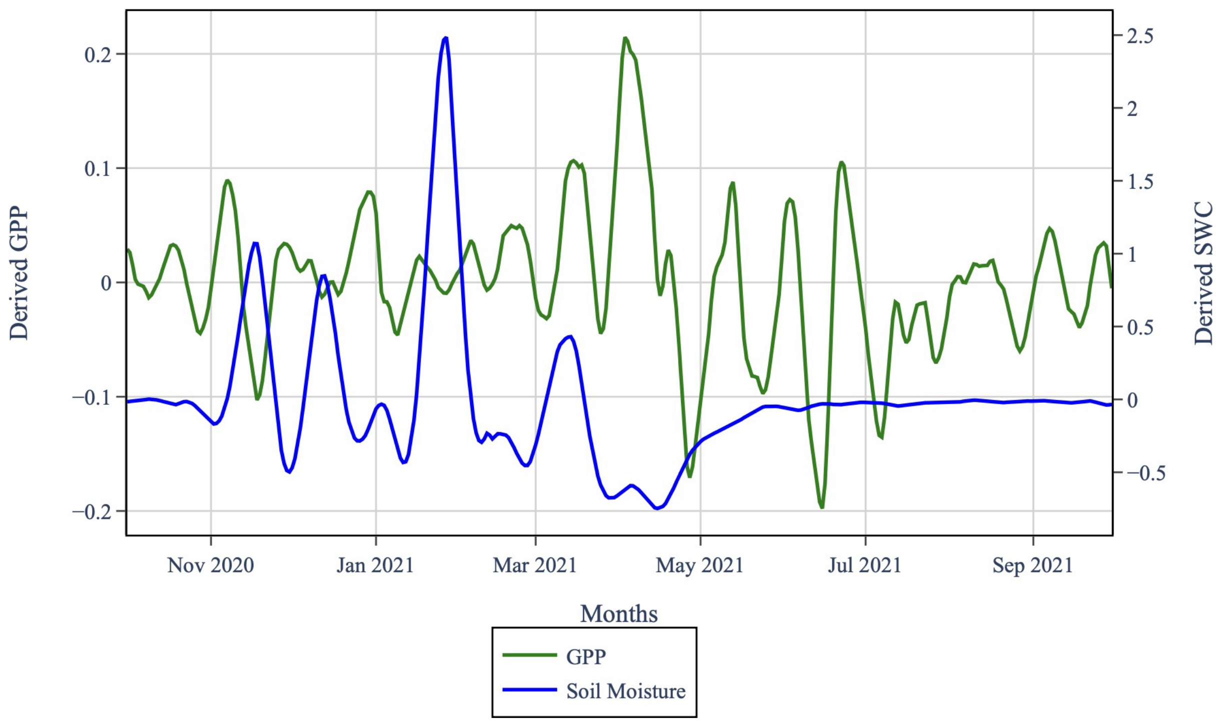

Figure 13. Smoothed time series using SSA over the dry year (WY2021) showing the dry-down timing of derived vegetation productivity (green) and derived soil moisture (blue) in an oak woodland savanna. Initial extreme soil dry-down period occurred at the end of January over 12 days similar to the second peak in March which lasted 13 days.

In a grassland

During the spring, I found from the cross-correlation analysis that soil moisture can lag up to 16 days in the wet year and 12 days in the dry year (Table 7). The Spearman's Rank correlation coefficients between SWC and GPP all became stronger and more significant once I applied the lag. There is an overall strong positive correlation between lagged SWC and GPP except for a weak positive correlation in 2019. The strongest correlations between lagged SWC and GPP occurred in the dry year.

Table 7. Cross-correlation results and Spearman's Rank correlation coefficients between soil moisture and lagged soil moisture with vegetation productivity. All relationships are significant at the 99% level except for the ones labeled as n.s.

Spring (March-May)	Lag days	SWC vs GPP	Lagged SWC vs GPP
2016	1	0.414	0.446
2017	16	0.327	0.702
2018	7	0.353	0.558
2019	3	0.0886 n.s.	0.271
2020	2	0.665	0.731
2021	12	0.707	0.781

During late spring, I found that the GPP response timing between the wet and dry year differed significantly. In the wet year, GPP dropped on May 3 and SWC dropped on April 7 (Figure 14). In the dry year, GPP dropped on April 2 and SWC dropped on March 14 (Figure 15).

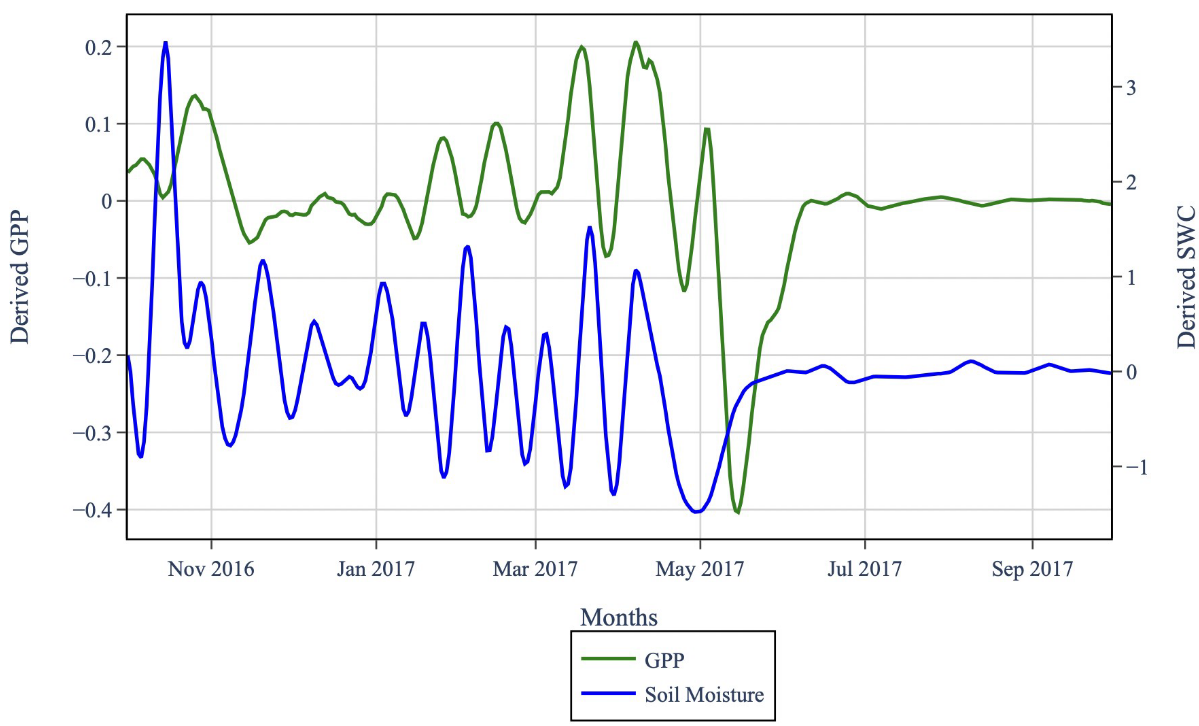

Figure 14. Smoothed time series over the wet year (2017) showing the dry-down timing of derived vegetation productivity (green) and derived soil moisture (blue) in a grassland. The dry-down period for GPP dropped in May and lasted 11 days.

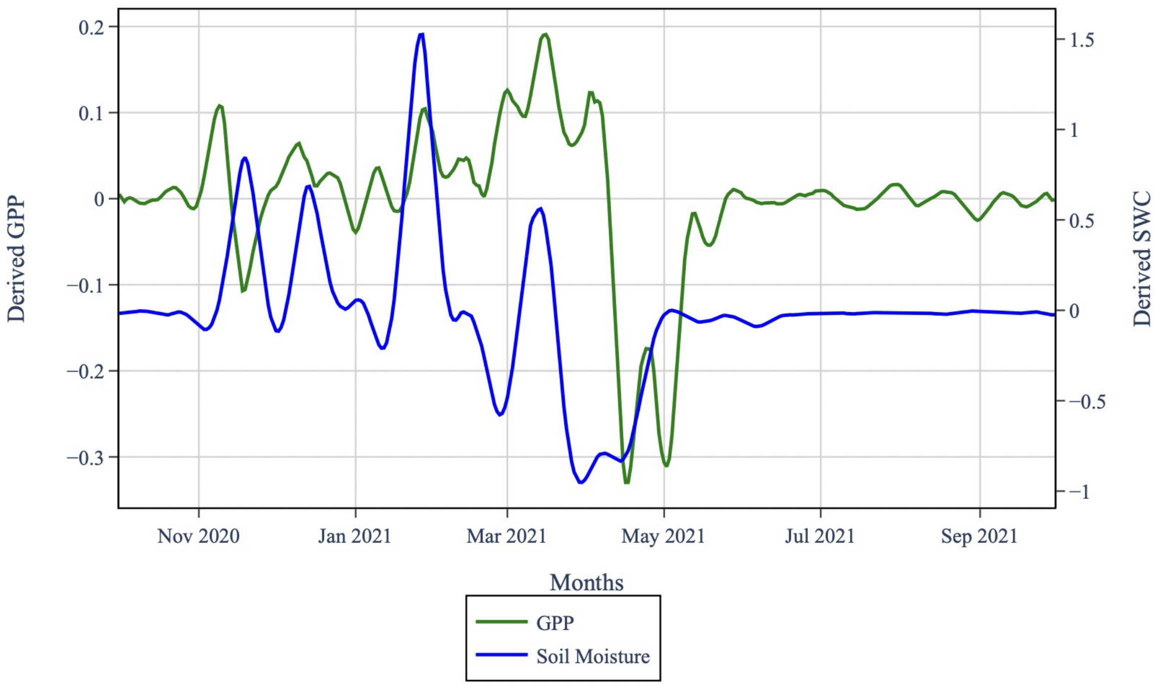

Figure 15. Smoothed time series over the dry year (2021) showing the dry-down timing of derived vegetation productivity (green) and derived soil moisture (blue) in a grassland. Initial extreme soil dry-down period occurred at the end of January over a month, while the second peak in March lasted a little over 2 weeks (16 days).

DISCUSSION

In this study, I demonstrate the variability and complexity of the relationship between soil moisture, vegetation productivity, and other environmental and biophysical variables. I found that LE and GPP were the most strongly linked variables when analyzing the relationship between energy balance variables and vegetation productivity. Moreover, I explored different MODIS products and their relationships to vegetation indices, as well as GPP maxima and seasonality in relation to soil moisture to understand the dynamics behind soil moisture and GPP using two different types of data. My main takeaway was that the oak woodland savanna ecosystem is more resilient to soil moisture changes, whereas the grassland was significantly less productive in the dry year. After investigating the GPP response timing in a wet and dry year, I observed that lagged SWC was strongly coupled with GPP in the spring, with the strongest coupling happening in the dry year. Finally, I found that the grasslands experience shorter growing seasons in the dry year where there is a rapid drop in GPP and significant dry-down of soil moisture occurring earlier in the dry year compared to the wet year. These findings are important for understanding the dynamic responses of these ecosystems to environmental changes and can help provide an updated high-level analysis for ecological management strategies aimed at maintaining ecosystem functioning and resistance of oak woodland savannas and grasslands in California.

Relationships of Energy Balance and Vegetation Productivity in an Oak Woodland Savanna and Grassland

I first explored the seasonal dynamics of energy balance and vegetation productivity (GPP) in an oak woodland savanna and grassland, focusing on the relationships between latent heat (LE), sensible heat (H), and other biophysical and environmental variables. In both the oak woodland savanna and the grassland, there was a strong positive relationship between LE and GPP, with high R^2 and Spearman's Rank correlation coefficients (Figure 4). This finding confirms that there is a consistent relationship between GPP and LE through time, as plants exchange carbon dioxide and water vapor through their stomata when photosynthesizing (Williams and Torn 2015). In the oak woodland savanna, LE and GPP both peaked during May in the wet year and April in the dry year, while in the grassland, both variables peaked in April for both wet and dry years. This earlier GPP maximum timing in the dry year in the oak savanna suggests that earlier in the year, soil moisture levels depleted at shallow depths when trees decrease evapotranspiration to prevent additional water loss (Liu et al. 2011). These differences support other studies that emphasize that vegetation types differentially control the energy partitioning in an ecosystem (Cicuéndez et al. 2023, Baldocchi et al. 2004). The similarities between the two ecosystem types may be due to the mixed vegetation present in the oak woodland savanna, where trees and grasses are present. Overall, these results confirm that the phenology of peak vegetation productivity and energy partitioning into latent heat is especially coupled in the growing season.

The relationship between soil moisture and different biophysical and environmental variables was generally consistent across both ecosystems (**Table 1**). In both the oak woodland savanna and the grassland, soil moisture showed a strong positive correlation with LE and a weaker relationship with H. Moreover, soil moisture displayed a strong negative correlation with vapor pressure deficit (VPD) in the grassland, but insignificant correlations in the oak woodland savanna. This suggests that the relationship between atmospheric moisture demand and soil water dynamics is much more evident in grasslands, which may be due to the mismatch in timing grasslands experience between the ideal temperatures and moisture conditions for plant growth. As temperatures increase, the atmospheric water demand (VPD) will increase and grasses are forced to begin evapotranspiration through stomatal conductance, further decreasing soil moisture available. Other studies confirm that soil moisture and VPD are strongly coupled through land-atmosphere interactions (Zhou et al. 2019, Stocker et al. 2018, Seneviratne et al. 2010).

Surprisingly, the grassland exhibited stronger positive correlations between soil moisture and GPP compared to the oak woodland savanna (Table 2, Table 3). Both ecosystems exhibit nonlinear relationships. This observation suggests that grassland productivity may be more sensitive to changes in soil moisture, potentially due to the shallower root systems and faster turnover rates of grasses compared to trees (Baldocchi et al. 2004). Moreover, other studies have shown that oak trees can perform well under adverse conditions where the trees' productivity can stay relatively stable due to their adaptive traits ideal for the Mediterranean climate, allowing GPP to be less directly linked to soil moisture levels (Gimeno et al. 2008). This may be due to the oak trees' ability to tap into deeper reserves of soil water when higher soil levels are depleted of water. The lack of a linear relationship between some variables, such as soil moisture and GPP, is explained by the presence of hysteresis, indicating that the relationship between these variables depends on the seasonal dynamics of rainfall and temperature ranges in each ecosystem (Hao et al. 2011). I conclude that energy balance and vegetation productivity are closely linked in both oak woodland savannas and grasslands, with latent heat playing a particularly important role in shaping these dynamics.

Relationships of Soil Moisture and Photosynthesis in an Oak Woodland Savanna and Grassland

The second question investigated the seasonal dynamics of soil moisture (SWC) and ecosystem-scale photosynthesis (GPP) in an oak woodland savanna and grassland, examining the differences in GPP maxima, the seasonality of GPP peaks, and relationships between environmental variables and various vegetation indices. During the wet year, I found that the oak woodland savanna had a higher GPP maximum compared to the grassland. (11.42 gC$m^{-2}d^{-1}$ and 8.46 gC m^{-2} d^{-1}, respectively). Interestingly, during the dry year the GPP maximum in the oak woodland savanna was lower than the grassland (6.13 gC$m^{-2}d^{-1}$ and 8.20 gC$m^{-2}d^{-1}$, respectively). This indicates that the oak woodland savanna generally assimilates more carbon than the grassland when water is available, consistent with previous findings of Mediterranean ecosystem functioning under drought conditions (Pereira et al. 2007). Moreover, the oak woodland savanna had a substantially higher total GPP assimilated over the growing season (434.76 gC $m^{-2}d^{-1}$ in the wet year and 348.96 gC $m^{-2}d^{-1}$ in the dry year) compared to the grassland (135.10 gC $m^{-2}d^{-1}$ in the wet year and 57.48 gC $m^{-2}d^{-1}$ in the dry year). This finding further confirms that the oak woodland savanna is generally more productive than the grassland ecosystem and less affected by soil moisture depletion (Baldocchi et al. 2004). Grasses are not robust to water stress and senesce when soil moisture is depleted in the ecosystem (Pereira et al. 2007).

Furthermore, I found that the oak woodland savanna exhibited distinct seasonality in GPP peaks; April was the peak month in drier years and May was the peak month in wetter years (Figure 8). The grassland consistently had GPP peaks in April across all years, with the exception of the wet year when it peaked in May (Figure 9). This difference in GPP seasonality highlights the varying sensitivities of the two ecosystems to water availability. More specifically, an earlier study argues that the seasonality of photosynthesis has more to do with rainfall timing and variability throughout the season than with the total amount of annual precipitation (Xu and Baldocchi 2003).

Moreover, I observed differing soil moisture dynamics in both ecosystems. In the oak woodland savanna, soil moisture levels in May of the wet year dropped from 30% on Day 1 to 5% on Day 30. Meanwhile, in the grassland, soil moisture levels in May 2017 dropped from 20% on Day 1 to 3% on Day 31, and in May 2021, soil moisture levels dropped from 5% on Day 1 to 4% on Day 22 (Figure 8, 10, 11). The small drop in May 2021 indicates that the soils in the grasslands had already dried out in April. Overall, this shows that grasses overall have earlier or shorter growing seasons in the study period in comparison to oak woodland savannas. These contrasting patterns highlight the divergent soil moisture dynamics in the two ecosystems, which can impact their productivity and resilience to changing water availability. Moreover, I found that the correlation of both ecosystems followed a sequential day order, similar to the findings of Baldocchi et al. 2004, where each point on the graph followed a chronological pattern through the course of the month (Figure 10). This demonstrates the strong seasonality of soil moisture to vegetation productivity during late spring when the soil dry-down period begins, especially for the grassland ecosystem.

In both the oak woodland savanna and grassland, relationships between MODIS products and vegetation indices were generally consistent across the years (Table 4, 5). GPP was positively correlated with LAI, fAPAR, and ET in both ecosystems, reflecting the close link between productivity and vegetation structure, function, and water use. Interestingly, there were no visible differences between wet and dry years in the relationship between the vegetation indices and MODIS products in the oak woodland savanna. This suggests that the vegetation may exhibit a high degree of resilience to interannual variability in precipitation inputs across a wide gradient. Alternatively, the changes that I observed from the eddy covariance data could not be measured from the satellite. Moreover, the strong relationship between the vegetation index VARI and fAPAR showed to be linearly related and strongly correlated in both ecosystems. This finding confirms what is known about water availability within a plant in relation to its photosynthetic potential seen through canopy greenness during the water years (Liu et al. 2011). In the grassland, the strongest relationships between SWC and GPP were observed during the wet and dry years in May, with April also showing a strong relationship. This highlights the importance of water availability in grassland productivity and indicates that the onset of the growing season is sensitive to changes in precipitation patterns. By comparison in the oak woodland, the only strong and significant relationship occurred in May of the wet year. I conclude that soil moisture and photosynthesis are closely linked in both oak woodland savannas and grasslands, with differences playing a particularly important role in shaping these dynamics.

Vegetation Productivity Response Timing in a Wet and Dry Year in an Oak Woodland Savanna and Grassland

The third question investigated the vegetation productivity response timing in wet and dry years in an oak woodland savanna and grassland. I analyzed the relationships between soil moisture and GPP while accounting for lags in soil moisture response specifically in the spring, from March to May. In both the oak woodland savanna and grassland, all correlations between soil moisture and GPP became stronger and more significant when incorporating lags. In the oak woodland savanna, soil moisture lagged up to 17 days in the wet year and 28 days in the dry year (Table 6). In the grassland, soil moisture lagged up to 16 days in the wet year and 12 days in the dry year (Table 7). These lag day findings were overall similar to a prior study that investigated the same two ecosystem types (Tonzi and Vaira) and calculated the lagged soil moisture from 2002-2006 (Liu et al. 2011). Additionally, the paper came to similar conclusions of annual grasslands presenting the most significant lag that is greatly controlled by the declining rate of soil moisture during the dry down period, when a 10-20 day lag is applied. I similarly found a similar lag day range for the 2016-2021 study period. These findings emphasize the importance of accounting for the temporal dynamics of soil moisture response when analyzing its relationship with GPP, and these temporal shifts can vary based on water availability.

In the oak woodland savanna and grassland, the drier years showed the strongest correlations between lagged soil moisture and GPP. A different paper investigating the controls and lags of soil carbon dioxide fluxes in 13 sites found that higher soil moisture values influence the intra-seasonal time lags with GPP (Vargas et al. 2010). This suggests that the strength of the relationship between soil moisture and GPP varies with water availability and that in drier years, GPP and lagged soil moisture are more tightly linked. I did not expect to see a negative correlation in 2019 when there was no lag in soil moisture during the spring, which could be due to other environmental or biophysical variable controls, such as light availability or specific extreme rainfall events, on the relationship that I did not take into account. Finally, the GPP response timing in late spring differed between the oak woodland savanna and grassland. In the oak woodland savanna, GPP and SWC dropped in close proximity during both wet and dry years, suggesting a relatively consistent response regardless of water availability (Figure 12, 13). However, in the grassland, the GPP response timing between the wet and dry years was significantly different, with the drop in GPP and SWC occurring earlier in the dry year compared to the wet year (Figure 14, 15). This result implies that grassland productivity is more sensitive to changes in water availability, likely due to rooting depth and resource strategies. Another study looking at the seasonal dynamics of lagged ecosystem responses of different water availability found that the grass litter in the second year of two consecutive wet springs can increase the respiration processes of a California oak-grass savanna, further emphasizing the significance of studying the response timing of vegetation productivity of an ecosystem (Ma et al. 2016).

Limitations and Future Directions

After discovering the importance of studying seasonal variability across different years, I conclude that the 6-year study period is not a sufficient temporal scale to fully understand the impact of soil moisture on vegetation productivity when focused on the interannual perspective. Studying a 15-year study period would include various wet and dry years, perhaps focusing on extreme droughts or precipitation anomalies, to make multiple comparisons instead of just the wet and dry year. The legacy effects year to year can provide a more in-depth analysis of time series data of terrestrial ecosystem functioning in relation to soil moisture availability over a longer time period. The interconnected behaviors of different environmental variables would be more accurately analyzed over a larger time period, but also through modeling or machine learning approaches, similar to the study conducted by Grant et. al 2011. Similar modeling studies include analyses on Net Ecosystem Exchange (NEE), Respiration, and solar radiation to gain more insight into the overall carbon cycling within an ecosystem and the photosynthetic behaviors that may be driven by seasonal temperature patterns, which is another limitation I experienced in my study approach. Focusing solely on productivity can be informative, but does not provide a full picture of how vegetation respiration is partitioned in relation to productivity in an ecosystem for varying soil moisture gradients. Additionally, the oak woodland savanna is a heterogeneous landscape and contains a less dense oak population, with an overstory of oak trees and an understory of grasses. I treated the oak woodland savanna as a homogeneous landscape within my data analyses, instead of separating the over and under the canopy for a more detailed comparison with the open annual grassland (Wang et al. 2016). Overall, partitioning a vegetation landscape into two different layers is complex and challenging. Ecosystem modeling would be a useful way of adding nuance to this specific ecosystem analysis, especially when focusing on soil rooting depths and differentiating the water acquisition strategies with the overstory and understory over a larger temporal scale.

CONCLUSIONS

In conclusion, this study provides a comparative analysis of the seasonal dynamics of soil moisture and vegetation productivity in an oak woodland savanna and a grassland ecosystem. The findings emphasize the differences in productivity, seasonality, and sensitivity to soil moisture between the two ecosystems, offering an updated analysis for understanding local ecosystem responses to environmental changes and further informing management strategies for preserving these ecosystems under future climate scenarios. In my paper, I highlight the importance of understanding how changes in climate, particularly precipitation patterns, may impact energy balance and vegetation productivity in these ecosystems. Moreover, I demonstrate that the seasonal dynamics of soil moisture and vegetation productivity are tightly linked in both oak woodland savannas and grasslands, with overall more productivity in the wet years. These results emphasize the importance of studying how climate change may influence the functioning of these ecosystems. Finally, the conclusions for my third question provide valuable observations of vegetation productivity response timing in wet and dry years in an oak woodland savanna and grassland, stressing the necessity of considering lags in soil moisture response when analyzing the relationship with vegetation productivity. Overall, my findings contribute to our understanding of how these ecosystems respond to fluctuations in water availability and can be applied to ecological management strategies for maintaining ecosystem functioning and resilience of oak woodland savannas and grasslands in California under more extreme climatic conditions driven by climate change. As more current studies develop, ecosystem management plans should be revised for these two Northern California ecosystems to preserve local biodiversity, prioritize ecosystem resistance to changing climate regimes, and protect wildlife and the well-being of all.

ACKNOWLEDGEMENTS

Thank you to everyone who has supported me through this thesis process. A huge thank you to my mentors Dave Miller, who supported me through countless meetings, difficult times, and thesis writing, and Trevor Keenan, who introduced me to ecosystem ecology and welcomed me into his lab allowing me to explore my passions surrounding terrestrial ecosystems. The support Patina Mendez and Danielle Perryman have provided me with over the past 2 years has been invaluable and I will always treasure the memories associated with ESPM 175. Thank you to my Slippery Scientist working group and ESPM175 friends for making me feel like I was not alone through this process. Last but not least, thank you to my parents for always being my rock, my friends who never got tired of hearing me talk about this project every other minute, and my dog for being my stress reliever. I dedicate this accomplishment to the memory of my beloved grandpa, Professor Ion Toderascu, who I know is always with me in spirit.

REFERENCES

About Ameriflux Data. 2022, July 2. https://ameriflux.lbl.gov/data/aboutdata/.

Appeears. NASA. https://appeears.earthdatacloud.nasa.gov/.

Baldocchi, D. D., Xu, L. & Kiang, N. 2004. How plant functional-type, weather, seasonal drought, and soil physical properties alter water and energy fluxes of an oak–grass savanna and an annual grassland. Agricultural and Forest Meteorology 123, 13–39.

Baldocchi, D., S. Y. Ma, and J. Verfaillie. 2020. On the inter- and intra-annual variability of ecosystem evapotranspiration and water use efficiency of an oak savanna and annual grassland subjected to booms and busts in rainfall. Global Change Biology 27.

Chapin, F. S., P. A. Matson, and H. A. Mooney. 2002. Principles of terrestrial ecosystem ecology. Springer, New York.

Chen, J., Y. Luo, J. Xia, K. Wilcox, J. Cao, X. Zhou, L. Jiang, S. Niu, K. Estera, R.-J. Huang, F. Wu, T. Hu, J. Liang, Z. Shi, J. Guo, and R.-W. Wang. 2017. Warming Effects on Ecosystem Carbon Fluxes Are Modulated by Plant Functional Types. Ecosystems 20:1–12.

Cicuéndez, V., J. Litago, V. Sánchez-Girón, C. Román-Cascón, L. Recuero, C. Saénz, C. Yagüe, and A. Palacios-Orueta. 2023. Dynamic relationships between gross primary production and energy partitioning in three different ecosystems based on eddy covariance time series analysis. Frontiers in Forests and Global Change 6:1017365.

Croft, H., J. M. Chen, N. J. Froelich, B. Chen, and R. M. Staebler. 2015. Seasonal controls of canopy chlorophyll content on forest carbon uptake: Implications for GPP modeling. Journal of Geophysical Research: Biogeosciences 120:1576–1586.

Gamon, J. A., C. B. Field, M. L. Goulden, K. L. Griffin, A. E. Hartley, G. Joel, J. Penuelas, and R. Valentini. 1995. Relationships Between NDVI, Canopy Structure, and Photosynthesis in Three Californian Vegetation Types. Ecological Applications 5:28–41.

Gherardi, L. A., and O. E. Sala. 2015. Enhanced interannual precipitation variability increases plant functional diversity that in turn ameliorates negative impact on productivity. Ecology Letters 18:1293–1300.

Gimeno, T. E., B. Pias, J. P. Lemos-Filho, and F. Valladares. 2008. Plasticity and stress tolerance override local adaptation in the responses of Mediterranean holm oak seedlings to drought and cold. Tree Physiology 29:87–98.

Grant, R. F., D. D. Baldocchi, and S. Ma. 2012. Ecological controls on net ecosystem productivity of a seasonally dry annual grassland under current and future climates: Modelling with ecosys. Agricultural and Forest Meteorology 152:189–200.

Hao, Y., H. Niu, Y. Wang, X. Cui, X. Kang, and J. Wang. 2011. Rainfall variability in ecosystem CO2 flux studies. Climate Research 46:77–83.

Huxman, T. E., K. A. Snyder, D. Tissue, A. J. Leffler, K. Ogle, W. T. Pockman, D. R. Sandquist, D. L. Potts, and S. Schwinning. 2004. Precipitation pulses and carbon fluxes in semiarid and arid ecosystems. Oecologia 141:254–268.

Jung, M., M. Reichstein, H. A. Margolis, A. Cescatti, A. D. Richardson, M. A. Arain, A. Arneth, C. Bernhofer, D. Bonal, J. Chen, D. Gianelle, N. Gobron, G. Kiely, W. Kutsch, G. Lasslop, B. E. Law, A. Lindroth, L. Merbold, L. Montagnani, E. J. Moors, D. Papale, M. Sottocornola, F. Vaccari, and C. Williams. 2011. Global patterns of land-atmosphere fluxes of carbon dioxide, latent heat, and sensible heat derived from eddy covariance, satellite, and meteorological observations. Journal of Geophysical Research 116:G00J07.

Liu, S., O. A. Chadwick, D. A. Roberts, and C. J. Still. 2011. Relationships between GPP, Satellite Measures of Greenness and Canopy Water Content with Soil Moisture in Mediterranean-Climate Grassland and Oak Savanna. Applied and Environmental Soil Science 2011:1–14.

MODIS Web. NASA. https://modis.gsfc.nasa.gov/data/.

Ma, S., D. Baldocchi, S. Wolf, and J. Verfaillie. 2016. Slow ecosystem responses conditionally regulate annual carbon balance over 15 years in Californian oak-grass savanna.

Agricultural and Forest Meteorology 228–229:252–264.

Mohammed, G. H. et al. 2019. Remote sensing of solar-induced chlorophyll fluorescence (SIF) in vegetation: 50 years of progress. Remote Sensing Environment 231, 111177.

Novick, K. A., D. L. Ficklin, P. C. Stoy, C. A. Williams, G. Bohrer, A. C. Oishi, S. A. Papuga, P. D. Blanken, A. Noormets, B. N. Sulman, R. L. Scott, L. Wang, and R. P. Phillips. 2016. The increasing importance of atmospheric demand for ecosystem water and carbon fluxes. Nature Climate Change 6:1023–1027.

O'Sullivan, M. et al. 2020. Climate-Driven Variability and Trends in Plant Productivity Over Recent Decades Based on Three Global Products. Global Biogeochemical Cycles 34.

Pereira, J. S., J. A. Mateus, L. M. Aires, G. Pita, C. Pio, J. S. David, V. Andrade, J. Banza, T. S. David, T. A. Paço, and A. Rodrigues. 2007. Net ecosystem carbon exchange in three contrasting Mediterranean ecosystems; the effect of drought. Biogeosciences 4:791–802.

Seneviratne, S.I., T. Corti, E.L. Davin, M. Hirschi, E.B. Jaeger, I. Lehner, B. Orlowsky, A.J. Teuling. 2010. Investigating soil moisture–climate interactions in a changing climate: A review." Earth-Science Reviews 99.3-4: 125-161.

Scott, R. L., E. A. Edwards, W. J. Shuttleworth, T. E. Huxman, C. Watts, and D. C. Goodrich. 2004. Interannual and seasonal variation in fluxes of water and carbon dioxide from a riparian woodland ecosystem. Agricultural and Forest Meteorology 122:65–84.

Stocker, T.F., D. Qin, G.-K. Plattner, M. Tignor, S.K. Allen, J. Boschung, A. Nauels, Y. Xia, Bex and P.M. Midgley. 2013. IPCC: Climate Change 2013: The Physical Science Basis. Contribution of Working Group I to the Fifth Assessment Report of the Intergovernmental Panel on Climate Change. Cambridge University Press, Cambridge, United Kingdom and New York, NY, USA, 1535 pp.

Stocker, B. D., J. Zscheischler, T. F. Keenan, I. C. Prentice, J. Peñuelas, and S. I. Seneviratne. 2018. Quantifying soil moisture impacts on light use efficiency across biomes. New Phytologist 218:1430–1449.

US-Ton: Tonzi Ranch- Ione. https://ameriflux.lbl.gov/sites/siteinfo/US-Ton

US-Var: Vaira Ranch- Ione. https://ameriflux.lbl.gov/sites/siteinfo/US-Var

Vargas, R., D. D. Baldocchi, M. F. Allen, M. Bahn, T. A. Black, S. L. Collins, J. C. Yuste, T. Hirano, R. S. Jassal, J. Pumpanen, and J. Tang. 2010. Looking deeper into the soil: biophysical controls and seasonal lags of soil CO_2 production and efflux. Ecological Applications 20:1569–1582.

Wang, J., X. Xiao, P. Wagle, S. Ma, D. Baldocchi, A. Carrara, Y. Zhang, J. Dong, and Y. Qin. 2016. Canopy and climate controls of gross primary production of Mediterranean-type deciduous and evergreen oak savannas. Agricultural and Forest Meteorology 226–227:132–147.

Williams, I. N., and M. S. Torn. 2015. Vegetation controls on surface heat flux partitioning, and land-atmosphere coupling. Geophysical Research Letters 42:9416–9424.

Xu, L., and D. D. Baldocchi. 2003. Seasonal trends in photosynthetic parameters and stomatal conductance of blue oak (Quercus douglasii) under prolonged summer drought and high temperature. Tree Physiology 23:865–877.

Zhou, S., A. P. Williams, A. M. Berg, B. I. Cook, Y. Zhang, S. Hagemann, R. Lorenz, S. I. Seneviratne, and P. Gentine. 2019. Land–atmosphere feedbacks exacerbate concurrent soil drought and atmospheric aridity. Proceedings of the National Academy of Sciences 116:18848–18853.

APPENDIX A

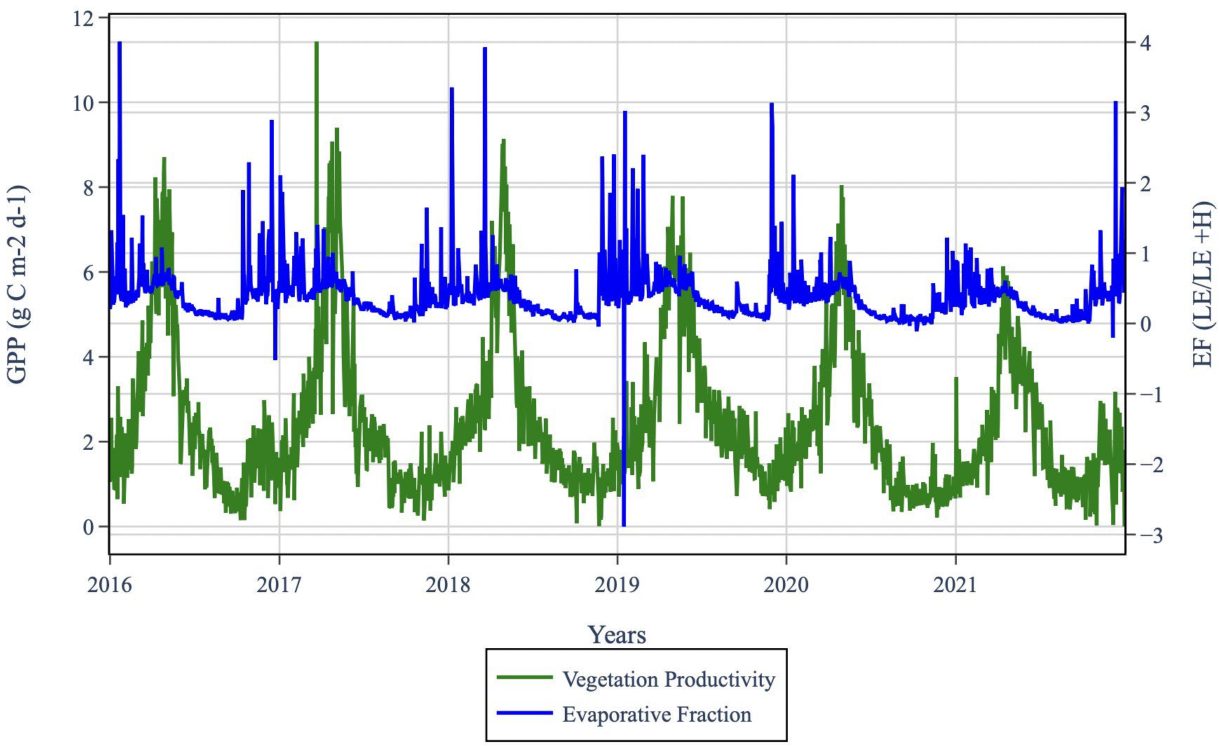

Figure A1. Seasonal oscillations observed by eddy covariance towers of daily-integrated daytime evaporative fraction (blue) and vegetation productivity (green) in the oak woodland savanna. Spikes in EF tend to occur during rain pulses in the ecosystem.

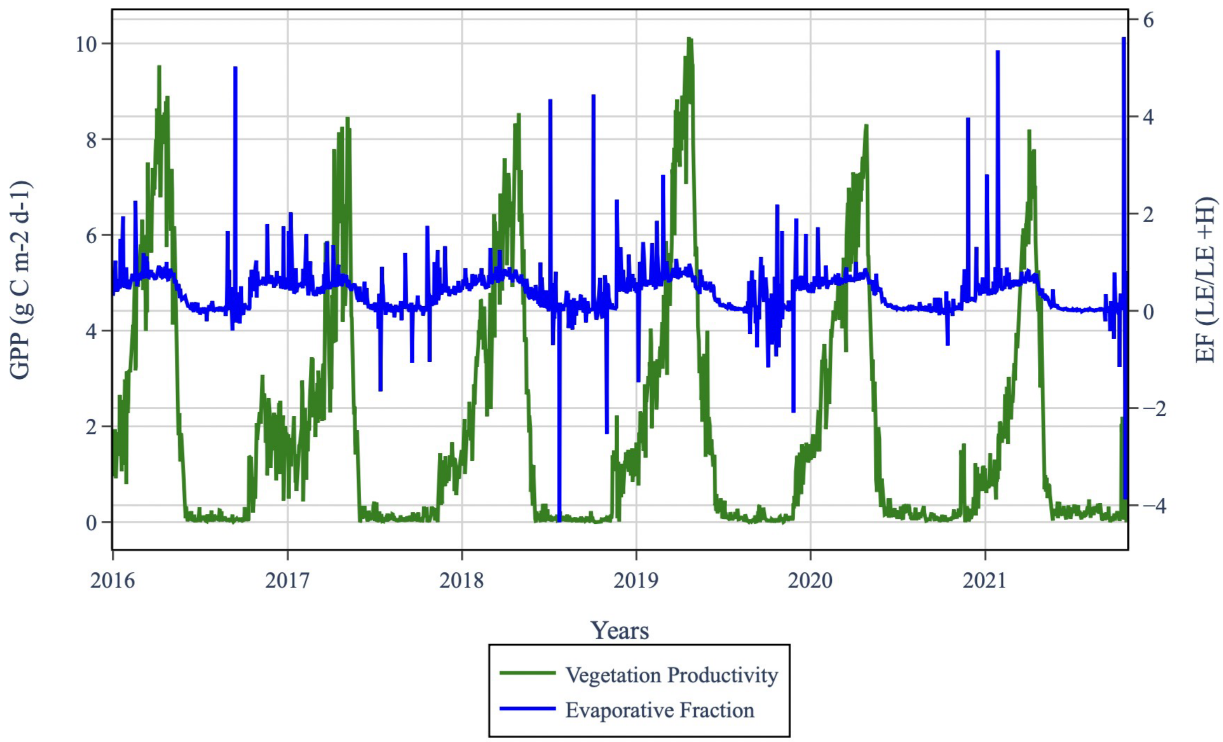

Figure A2. Seasonal oscillations observed by eddy covariance towers of daily-integrated daytime evaporative fraction (blue) and vegetation productivity (green) in the grassland. Spikes in EF tend to occur during rain pulses in the ecosystem.

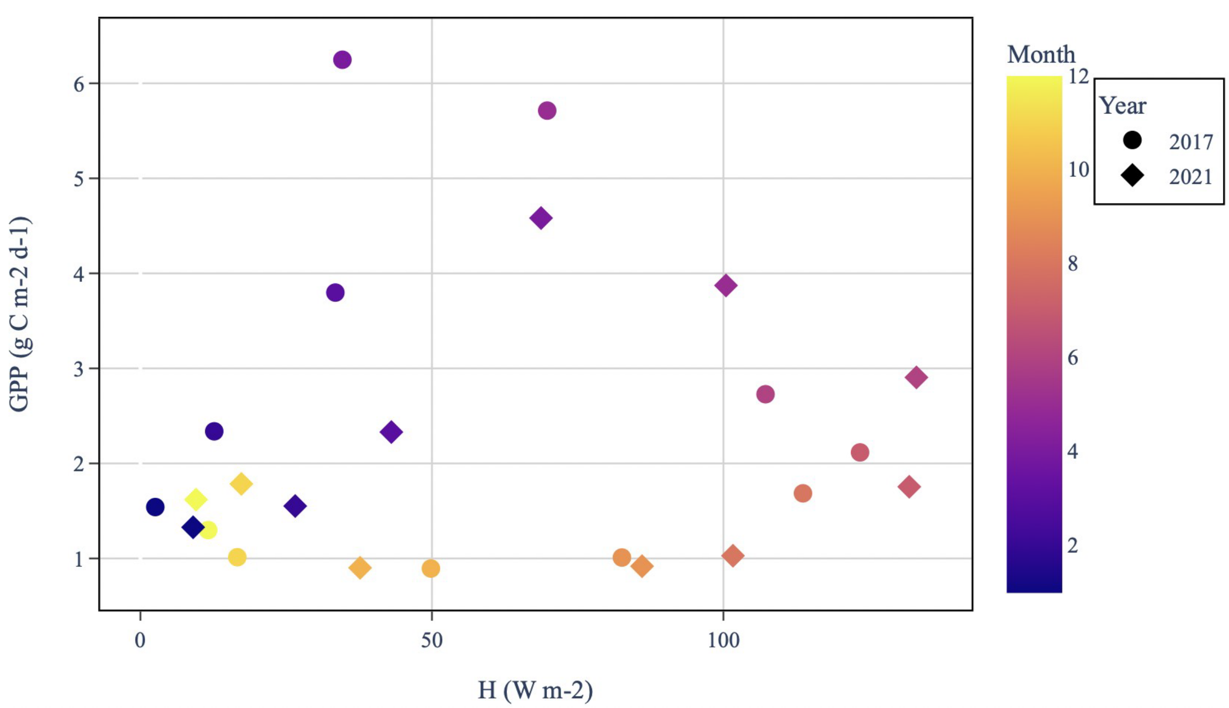

Figure A3. Oak woodland savanna seasonal dynamics of the relationship between monthly aggregated sensible heat (H) and gross primary production (GPP) in the wet (2017) and dry (2021) years. Follows a hysteresis shape.

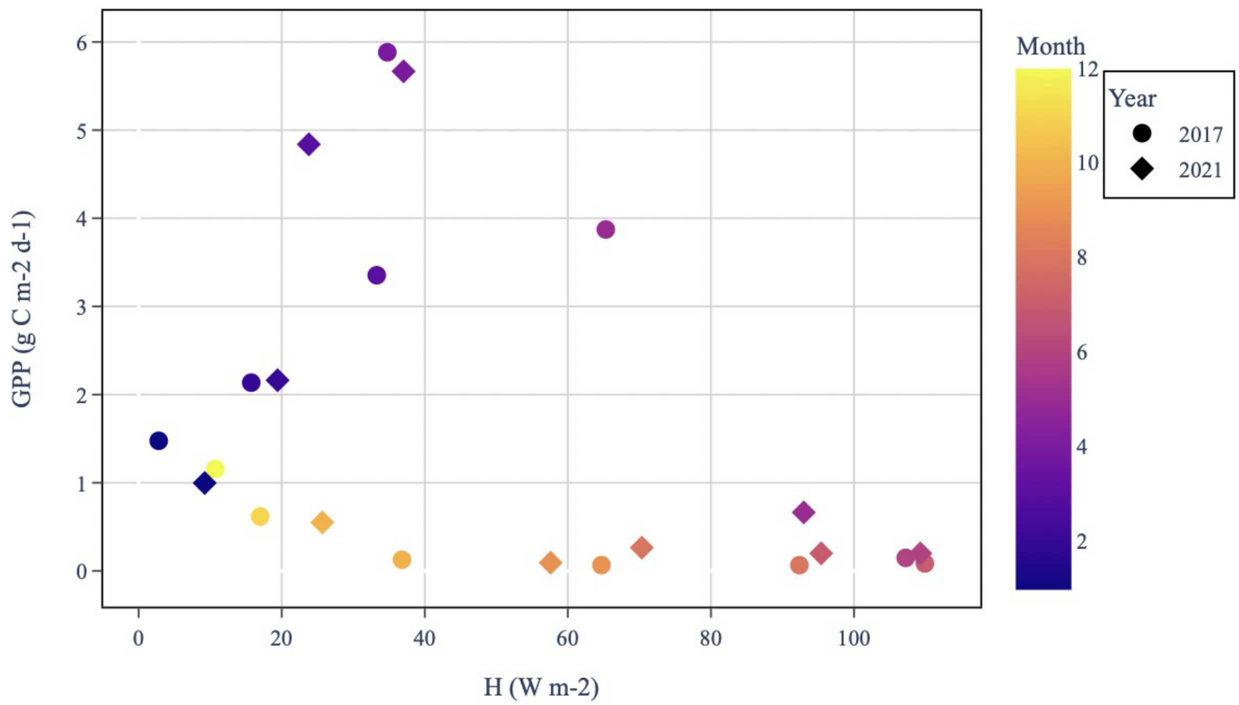

Figure A4. Grassland seasonal dynamics of the relationship between monthly aggregated sensible heat (H) and gross primary production (GPP) in the wet (2017) and dry (2021) years. Follows a hysteresis shape.

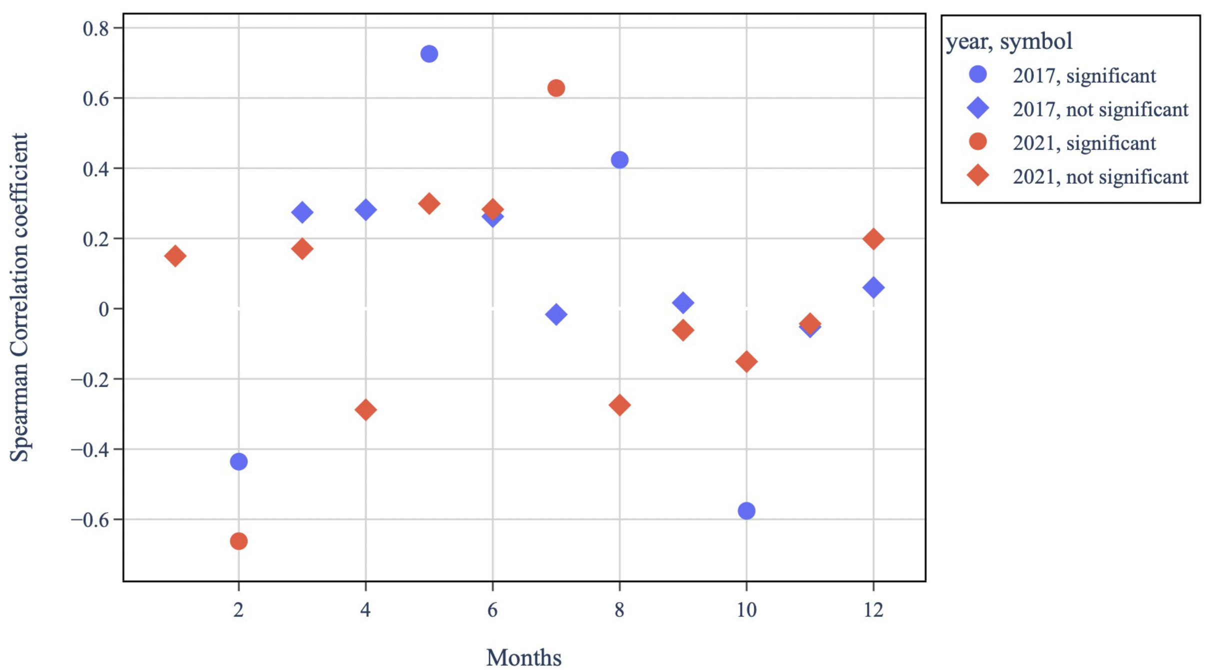

Figure A5. Spearman's Rank correlation coefficient values in oak woodland savanna between soil water content (SWC) and gross primary production (GPP) in the wet (2017) and dry (2021) years. Significance under 95% confidence level, most positive correlation in May 2017.

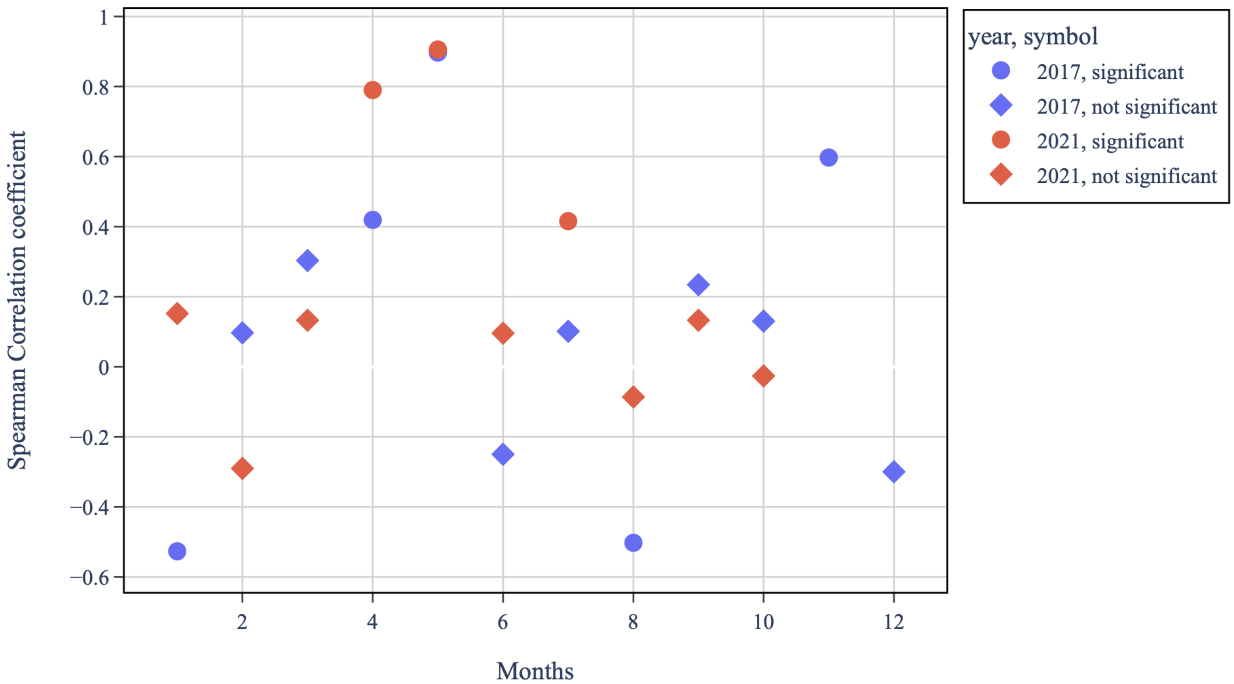

Figure A6. Spearman's Rank correlation coefficient values in grassland between soil water content (SWC) and gross primary production (GPP) in the wet (2017) and dry (2021) years. Significance under 95% confidence level, most positive correlations in May 2017 and 2021.

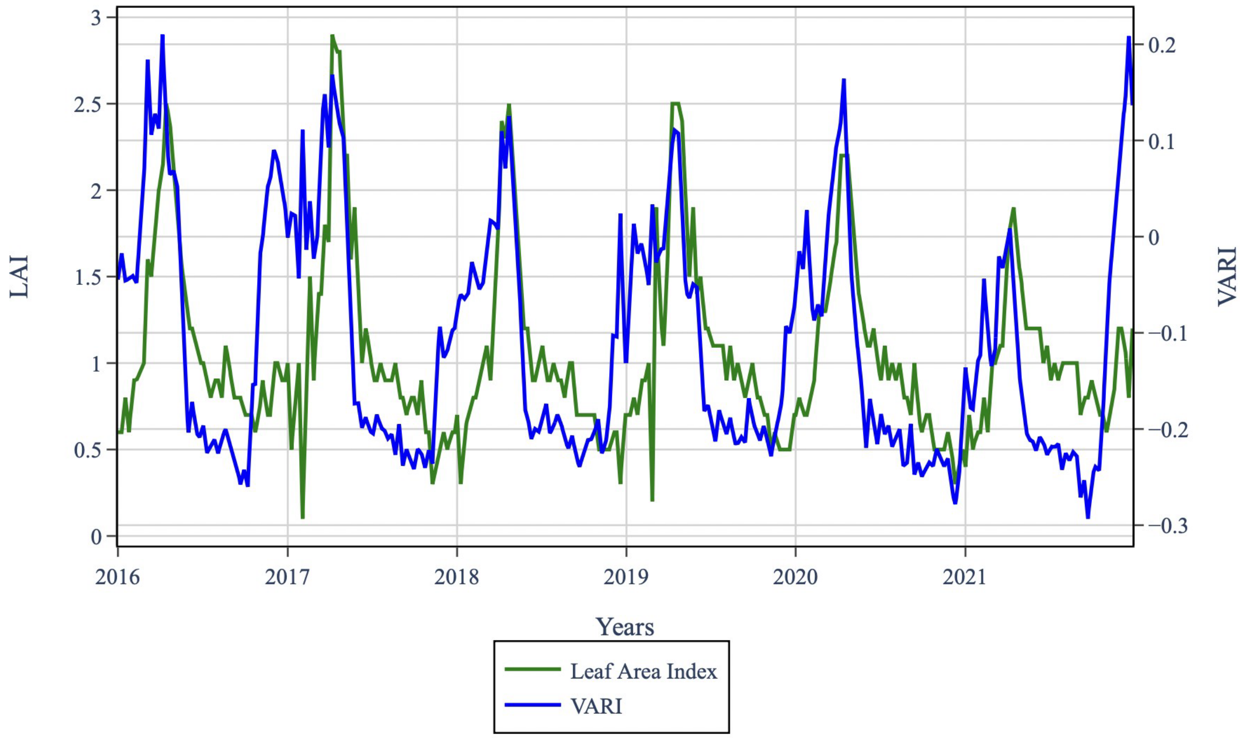

Figure A7. Linearly interpolated seasonal oscillations of Leaf Area Index (LAI, green) and Visible Atmospherically Resistant Index (VARI, blue) in the oak woodland savanna via MODIS sensor.

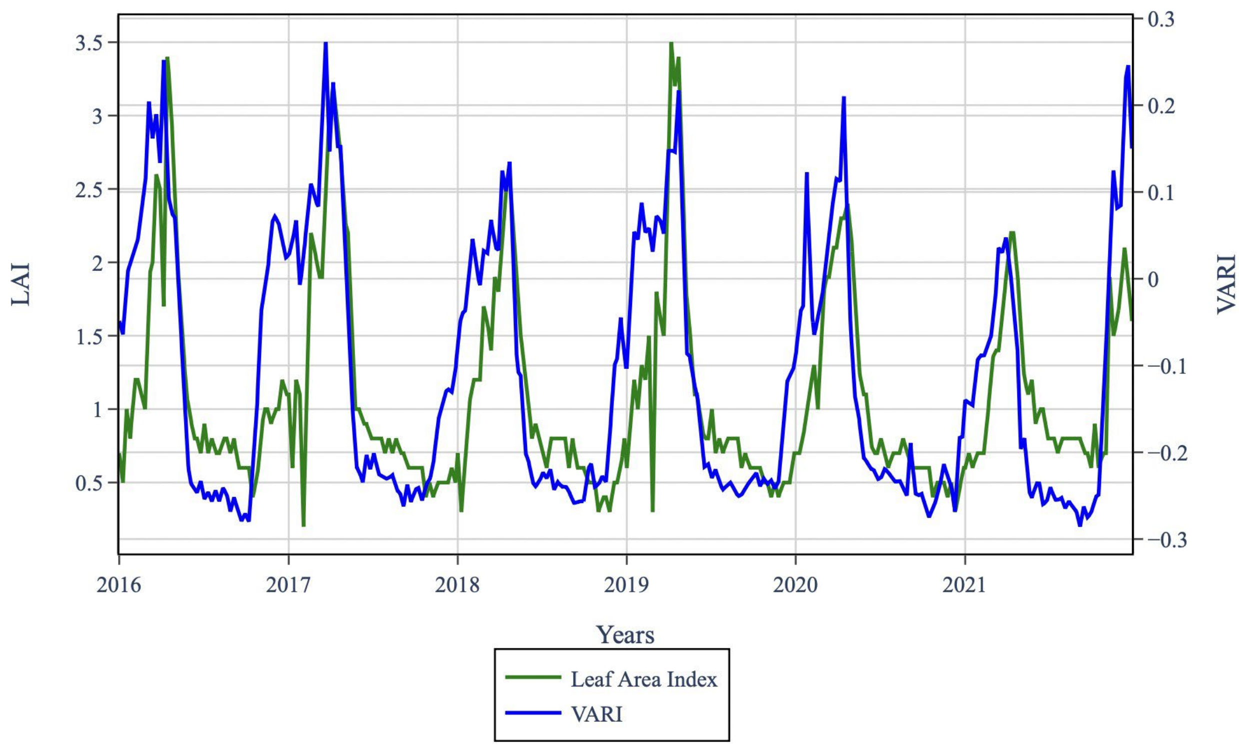

Figure A8. Linearly interpolated seasonal oscillations of Leaf Area Index (LAI, green) and Visible Atmospherically Resistant Index (VARI, blue) in the grassland via MODIS sensor.

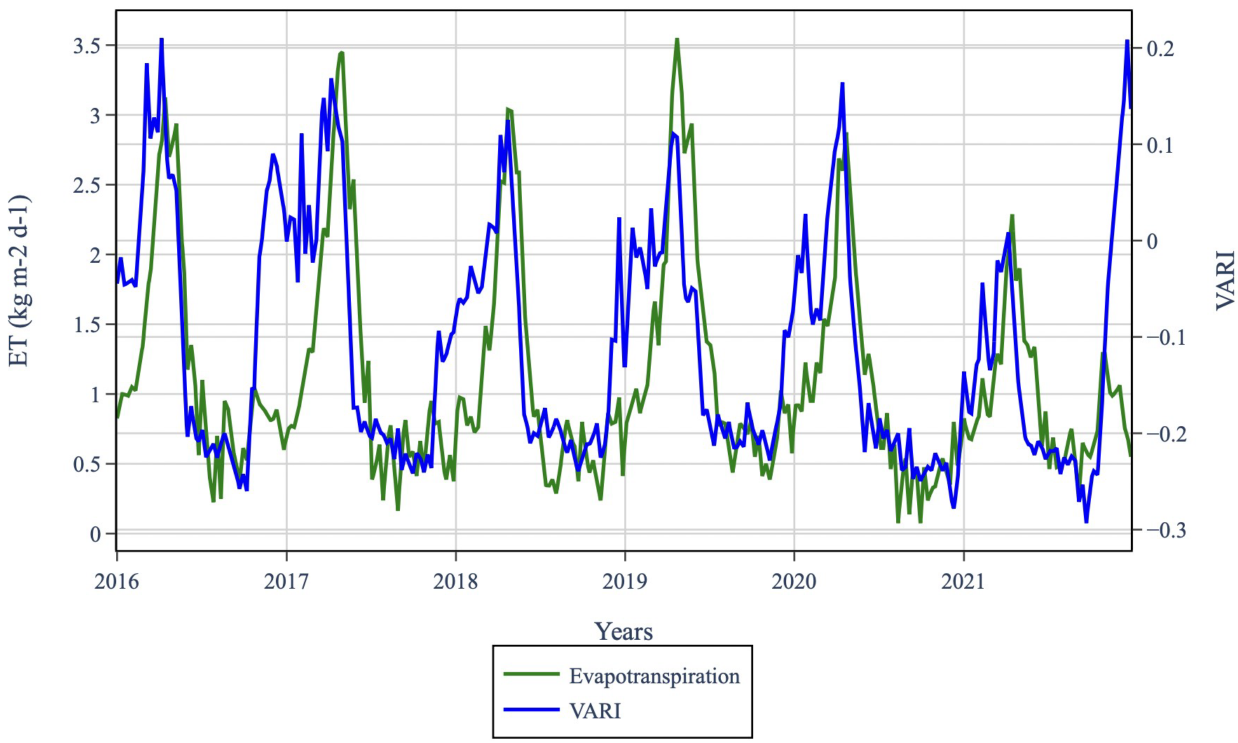

Figure A9. Linearly interpolated seasonal oscillations of Evapotranspiration (ET, green) and Visible Atmospherically Resistant Index (VARI, blue) in the oak woodland savanna via MODIS sensor.

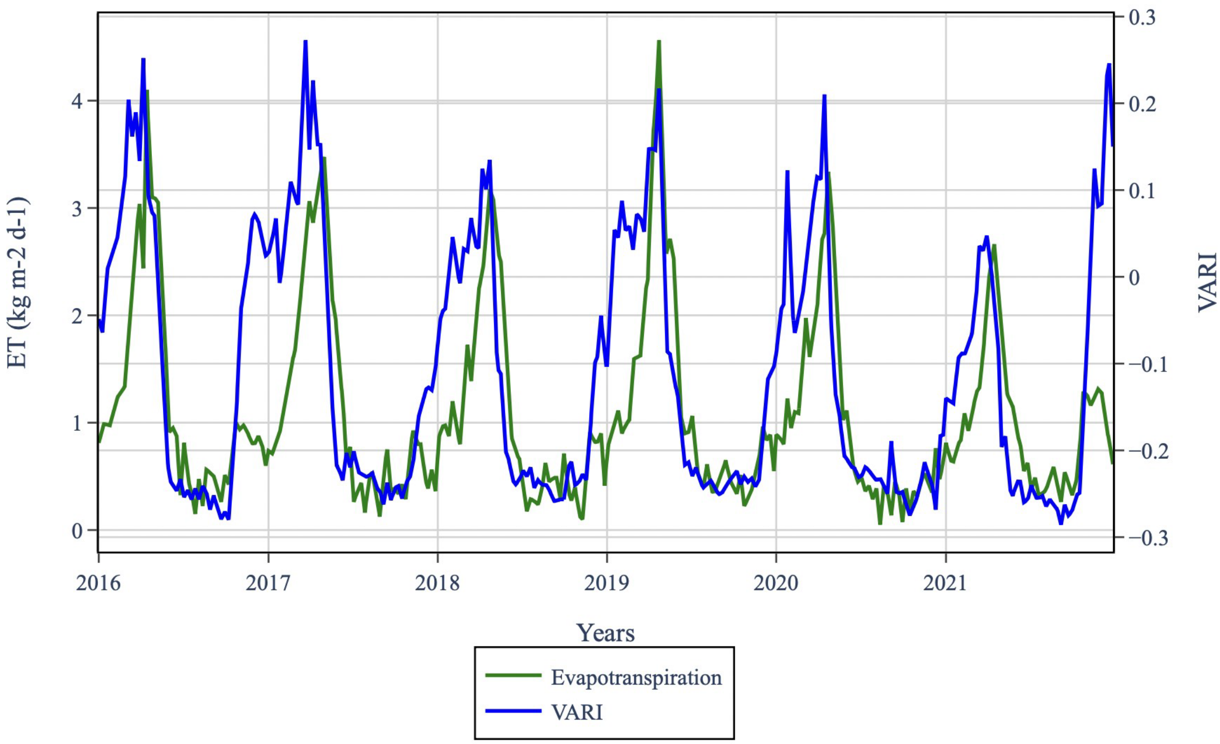

Figure A10. Linearly interpolated seasonal oscillations of Evapotranspiration (ET, green) and Visible Atmospherically Resistant Index (VARI, blue) in the grassland via MODIS sensor.

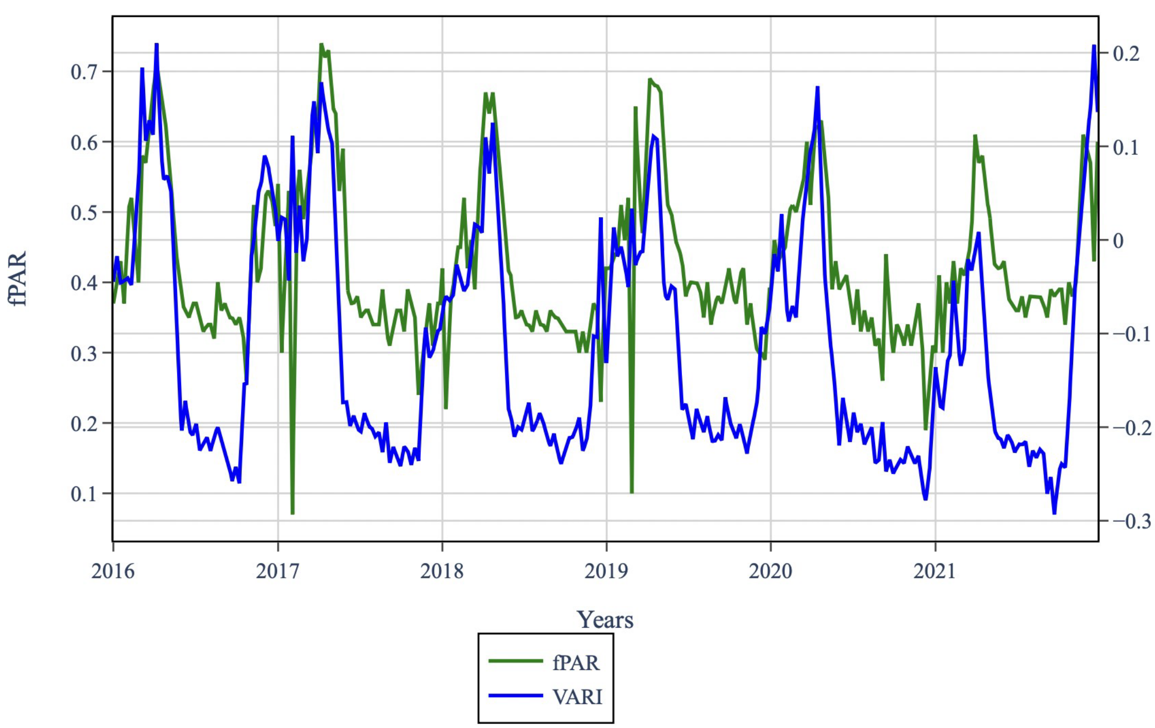

Figure A11. Linearly interpolated seasonal oscillations of fraction of Absorbed Photosynthetically Active Radiation (fAPAR, green) and Visible Atmospherically Resistant Index (VARI, blue) in the oak woodland savanna via MODIS sensor.

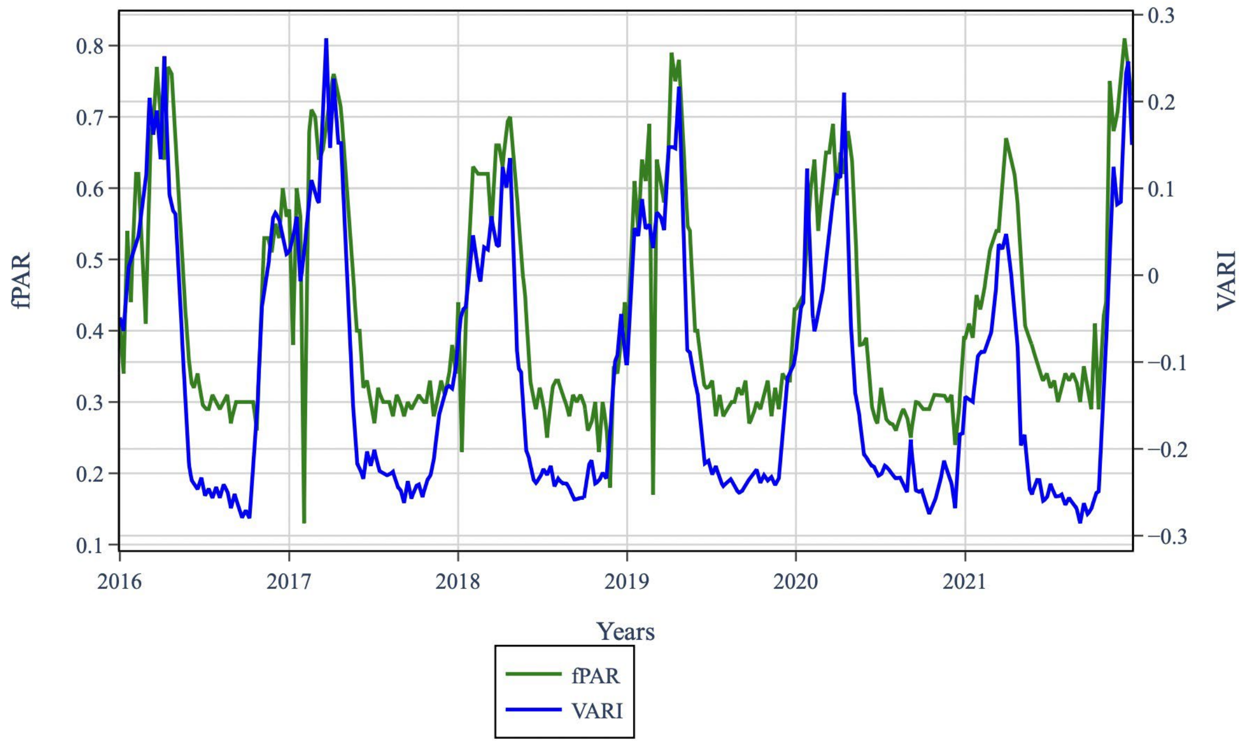

Figure A12. Linearly interpolated seasonal oscillations of fraction of Absorbed Photosynthetically Active Radiation (fAPAR, green) and Visible Atmospherically Resistant Index (VARI, blue) in the grassland via MODIS sensor.

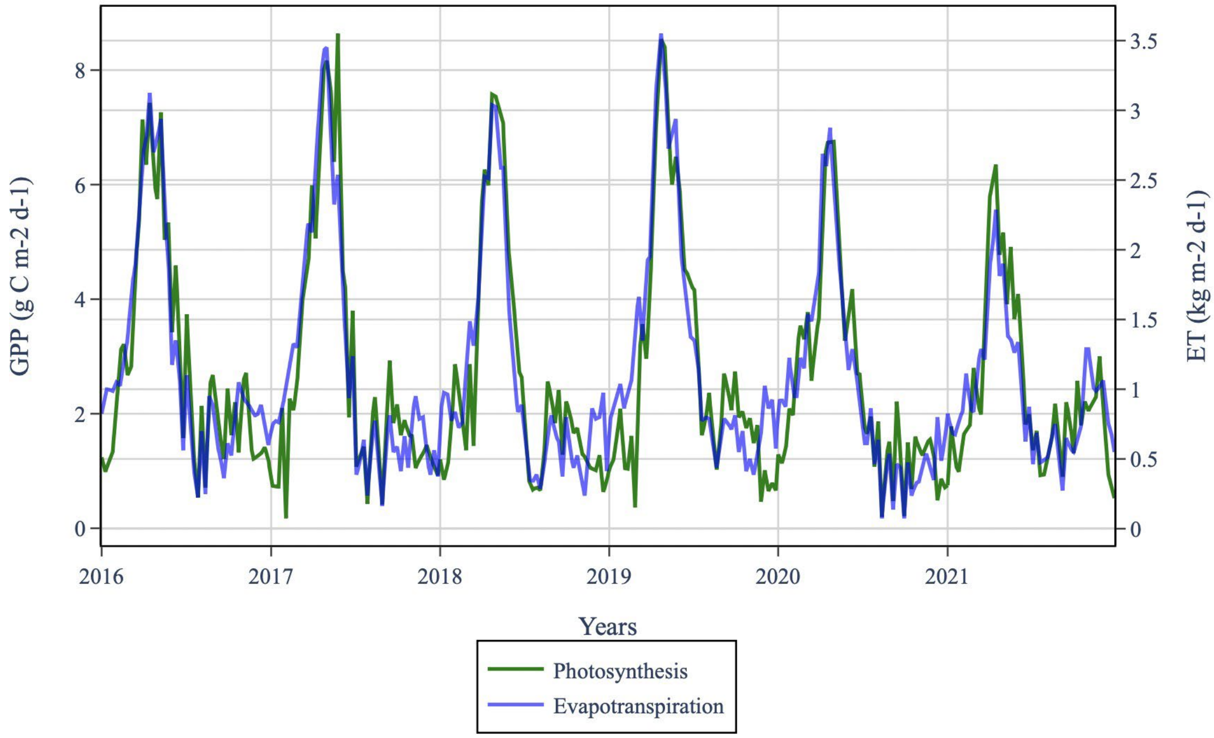

Figure A13. Linearly interpolated seasonal oscillations of photosynthesis (GPP, green) and Evapotranspiration (ET, blue) in the oak woodland savanna via MODIS sensor.

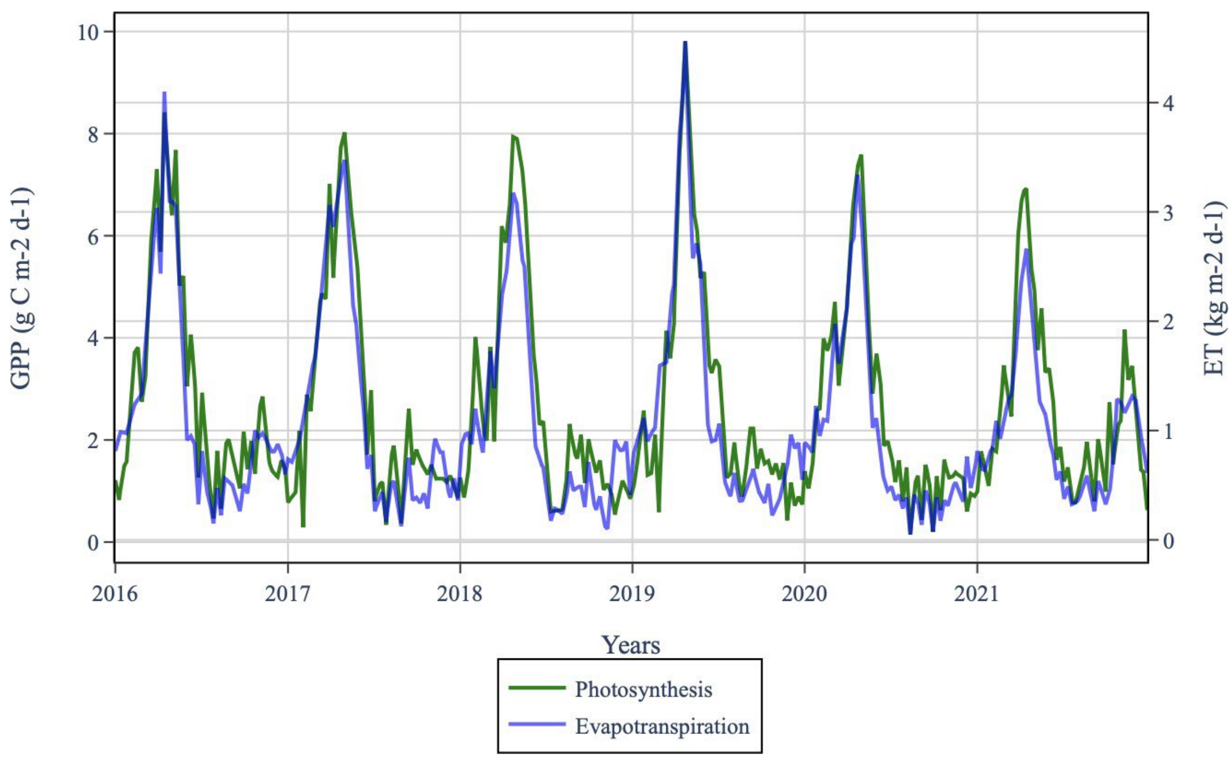

Figure A14. Linearly interpolated seasonal oscillations of photosynthesis (GPP, green) and Evapotranspiration (ET, blue) in the grassland via MODIS sensor.